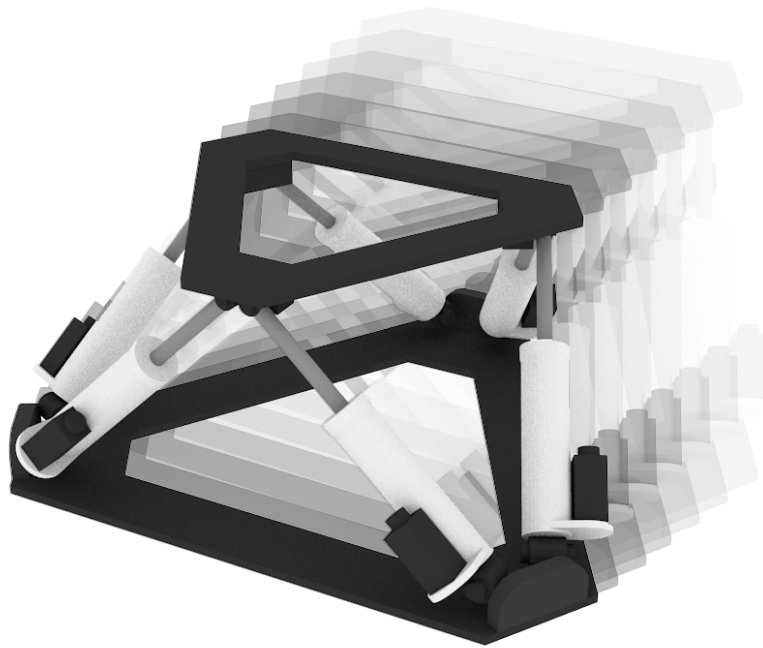


CHALMERS



PREPOSITIONING OF A DRIVING SIMULATOR MOTION SYSTEM

A Predictive Motion Cueing Algorithm

Master's thesis in Systems, Control and Mechatronics

PATRIK HANSSON
ANDERS STENBECK

Department of Applied Mechanics
Division of Vehicle Engineering & Autonomous Systems
CHALMERS UNIVERSITY OF TECHNOLOGY
Göteborg, Sweden 2014
Master's thesis 2014:20

MASTER'S THESIS IN SYSTEMS, CONTROL AND MECHATRONICS

PREPOSITIONING OF A DRIVING
SIMULATOR MOTION SYSTEM

A Predictive Motion Cueing Algorithm

PATRIK HANSSON
ANDERS STENBECK

Department of Applied Mechanics

Division of Vehicle Engineering & Autonomous Systems

CHALMERS UNIVERSITY OF TECHNOLOGY

Göteborg, Sweden 2014

PREPOSITIONING OF A DRIVING
SIMULATOR MOTION SYSTEM
A Predictive Motion Cueing Algorithm
PATRIK HANSSON
ANDERS STENBECK

© PATRIK HANSSON, ANDERS STENBECK, 2014

Master's thesis 2014:20
ISSN 1652-8557
Department of Applied Mechanics
Division of Vehicle Engineering & Autonomous Systems
Chalmers University of Technology
SE-412 96 Göteborg
Sweden
Telephone: +46 (0)31-772 1000

Cover:
A 3D sketch of a motion system similar to the one used in the VTI Sim IV driving simulator. Model created in Blender.

Chalmers Reproservice
Göteborg, Sweden 2014

PREPOSITIONING OF A DRIVING
SIMULATOR MOTION SYSTEM
A Predictive Motion Cueing Algorithm
Master's thesis in Systems, Control and Mechatronics
PATRIK HANSSON
ANDERS STENBECK
Department of Applied Mechanics
Division of Vehicle Engineering & Autonomous Systems
Chalmers University of Technology

ABSTRACT

Every dynamic driving simulator, no matter how advanced its motion system is, has limited space in which to recreate the accelerating motions of the simulated road vehicle. The VTI driving simulator Sim IV is no exception. The classic motion cueing algorithm used in Sim IV strives to centre the drivers cabin in the simulator motion envelope and is tuned to precisely accommodate accelerations in a worst case scenario without hitting the physical boundaries. Using knowledge about the road ahead and the vehicle model one can preposition the cabin to an off-centre point, virtually increasing the available space so that larger motions are made possible. This aims to increase the impression of realism in the driving experience. The prepositioning algorithm presented in this thesis is developed as an addition to the current motion cueing algorithm and make use of road- and vehicle data to find a suitable preposition. The motion to the preposition is made under the human perception threshold to avoid rendering of false cues. Simulations show that the amount of acceleration presented by the sled can, with prepositioning, be increased by up to 25% in longitudinal and 53% in lateral direction. During a comparative study of the simulator motion, test subjects indicated that they had a more realistic driving experience with than without prepositioning.

Keywords: driving simulator, motion cueing, prepositioning

SAMMANFATTNING

Varje dynamisk körsimulator, oavsett hur avancerat dess rörelsesystem är, har ett begränsat utrymme inom vilken den kan återskapa de rörelserna från den simulerade fordonsmodellen. VTI:s körsimulator Sim IV är inget undantag. Den klassiska motion cueing-algoritmen som används i Sim IV strävar efter att centrera förarhytten och är inställd för att hantera accelerationer i ett värstafallsscenario utan att nå sina fysiska gränser. Med information om vägen framför och om fordonsmodellen kan man förpositionera förarhytten till en excentrisk punkt för att utöka rörelseutrymmet och på så sätt tillåta större rörelser. Detta för att öka känslan av realism i körningen. Förpositioneringsalgoritmen som presenteras i detta examensarbete är utvecklat som ett tillägg till nuvarande motion cueing-algoritm och använder sig utav väg- och fordonsdata för att hitta en passande förposition. Rörelsen fram till förpositionen sker under den mänskliga perceptionströskeln för att förhindra att så kallade "false cues" uppstår. Simuleringar visar att när prepositionering används kan andelen acceleration som presenteras i släden ökas med upp till 25% i longitudinell ledd (längs med fordonet) och 53% i lateral ledd (tvärs fordonet). Under ett jämförande test i simulatorn indikerade försökspersoner att de hade en mer realistisk körupplevelse med än utan prepositionering.

ACKNOWLEDGEMENTS

In the effort of writing this masters thesis we, the authors, would like to show gratitude towards our examiner Fredrik Bruzelius, instructor Artem Kusachov and colleague and simulator expert Bruno Augusto for accepting us as thesis students and guiding us through the process.

Thanks also to thank Martin Fischer for both his thorough work with the motion cueing algorithm upon which we based our work, and for discussing ideas. Also Carl Sandberg has been helpful discussing ideas. A special thanks to all the people at VTI for their hospitality. Thanks also to all the test subjects who, without compensation, came and evaluated our work.

We also would like to take the opportunity to thank our respective families for all their support during the whole study period.

Fredrik, Artem, Bruno, Martin, Calle, VTI staff, test subjects and our families, thanks a lot.

Göteborg, June 30, 2014

PATRIK HANSSON & ANDERS STENBECK

NOMENCLATURE

Glossary

<i>Dynamic simulator</i>	a simulator with motion capabilities.
<i>False cue</i>	unwanted rendering of motion as a result of poor motion cueing or unexpected driving behaviour.
<i>Heave</i>	linear motion along the z -axis.
<i>Hexapod</i>	six linear actuators arranged to allow a motion system six degrees of freedom, a.k.a. Gough-Stewart platform.
<i>Jerk</i>	the time derivative of acceleration.
<i>Motion cueing algorithm</i>	a system of filters used to translate accelerations generated by the simulated vehicle model to be presented to the driver in the limited motion envelope of a simulator
<i>Motion envelope</i>	the limited volume spanned by the boundaries of motion in a dynamic simulator.
<i>Motion system</i>	the motion platform and respective control systems in the simulator.
<i>PD controller</i>	proportional-derivative loop feedback controller.
<i>Pitch</i>	rotation around the y -axis, denoted θ .
<i>Roll</i>	rotation around the x -axis, denoted ϕ .
<i>Sim IV</i>	the VTI 8-DOF driving simulator in Göteborg, Sweden.
<i>Surge</i>	linear motion along the x -axis.
<i>Sway</i>	linear motion along the y -axis.
<i>Test suite</i>	software validation test environment
<i>Tilt coordination</i>	the method of using gravity to trick a human into thinking he/she accelerates horizontally.
<i>Vestibular system</i>	motion sensitive organs in the inner ear.
<i>Washout filter</i>	a filter which make the motion system return to its neutral position.
<i>x,y-sled</i>	horizontal motion envelope-expanding construction.
<i>Yaw</i>	rotation around the z -axis, denoted ψ .

Abbreviations

DOF	degrees of freedom
LCD	liquid crystal display
MCA	motion cueing algorithm
MS	motion system
PP	prepositioning
RMS	root mean square
TC	tilt coordination
VTI	the Swedish National Road and Transport Research Institute

Capital letters

C	curvature [1/m]
H	high pass filter
R	radius (of road curve) [m]
T	torque [Nm]

Lower case Letters

a	acceleration [m/s ²]
d	displacement [m]
g	gear ratio alt. gravity acceleration, ≈ 9.81 [m/s ²]
j	jerk [m/s ³]
m	mass [kg]
r	radius (of wheel) [m]
t	time [s]
v	velocity [m/s]

Greek letters

β	orientation
η	efficiency
θ	pitch, rotation about y -axis [rad]
ϕ	roll, rotation about x -axis [rad]
ψ	yaw, rotation about z -axis [rad]
ω	rotational velocity [rad/s]

Subscripts

\square_{Bd}	boundary
\square_e	engine
\square_f	fixed
\square_h	horizon
\square_{Hx}	hexapod
\square_{lf}	low frequency (used with filter)
\square_{lim}	limit
\square_{mf}	middle frequency (used with filter)
\square_{nom}	nominal
\square_n	normal
\square_{ref}	reference
\square_s	sample
\square_{Sd}	sled
\square_{TC}	tilt coordination
\square_{Vh}	vehicle model

CONTENTS

Abstract	i
Sammanfattning	ii
Acknowledgements	iii
Nomenclature	v
Contents	ix
1 Introduction	1
1.1 Problem formulation	1
1.2 Purpose	2
1.3 Previous work	2
1.4 Method	2
1.5 Limitations	3
1.6 Main results	3
2 Driving simulators	4
2.1 Simulator types	4
2.2 Motion-base driving simulators	4
3 Motion Cueing	6
3.1 Human motion sensing physiology	6
3.1.1 Vestibular system	6
3.2 Tilt Coordination	7
3.3 Washout filters	8
3.3.1 Classical washout algorithm	8

3.3.2	Adaptive washout filter	8
3.3.3	Optimal washout filter	9
4	Sim IV	10
4.1	Motion Cueing in Sim IV	10
5	Prepositioning	13
5.1	Velocity dependent, longitudinal prepositioning	14
5.1.1	Vehicle model	14
5.1.2	Longitudinal prepositioning algorithm	16
5.2	Road and velocity dependent, lateral prepositioning	17
5.2.1	Data collection	18
5.2.2	Lateral prepositioning algorithm	19
5.3	Acceleration and jerk limitation	21
5.4	Expanding the motion envelope	24
5.5	Implementation	25
5.6	Safety	26
6	Results	28
6.1	Simulation results	28
6.1.1	Tests of longitudinal prepositioning	29
6.1.2	Tests of lateral prepositioning	34
6.1.3	Test of total prepositioning	37
6.2	Initial test drives	37
6.3	Study	39
7	Discussion	41
	References	43

Appendix A Test road "Curvy test track"	45
Appendix B Test road "Swedish rural road"	46
Appendix C Test run profiles	47
Appendix D Parameter settings	50
Appendix E Questionnaire	51
Appendix F Study results	52
Appendix G Images	53

1 Introduction

VTI, the "Swedish National Road and Transport Research Institute" is an independent research institute that conducts research in the transport sector. VTI performs research related to infrastructure, traffic and transport. To better understand human behaviour and their interaction with the transport system in a safe environment VTI deploys several advanced driving simulators. The most advanced in terms of motion technology is Sim IV located in Göteborg [1].

The VTI Sim IV is an 8-DOF (6+2 degrees of freedom) driving simulator capable of simulating a drivers environment for either a car or a truck. During simulation the movements of a vehicle model are recreated by a motion system to give the driver a realistic driving experience. The Sim IV motion system is built around six linear actuators called a hexapod or Gough-Stewart platform, which is capable of moving the drivers cabin in 6-DOF, translation x, y, z and rotation ϕ, θ, ψ . The hexapod has natural limitations in both its translational and rotational motion and is therefore placed on top of a platform capable of much larger translational movements, a so called x,y -sled. Thus the two redundant (+2) degrees of freedom. Sim IV is described in more detail in Chapter 4.

Due to the physical limitations of the simulators motion system a motion cueing algorithm (MCA) is needed in order to achieve a realistic driving experience while keeping the simulator within its spatial limitations, the motion envelope. The MCA, described in detail in Chapter 3, translates the accelerations produced by the vehicle model to the driver via the actuators in the motion system. Some sustained linear accelerations are represented with so called tilt coordination (TC).

1.1 Problem formulation

Even though Sim IV, thanks to its x,y -sled, has a relatively large motion envelope it is limited in comparison with a real vehicle. Further limitations arise due to the nature of the MCA washout which strives to return the driver's cabin to a neutral centre position in preparation for rendering of all possible manoeuvres. The drawback of this solution is that only a part of the available space used for linear accelerations by the x,y -sled is available in every direction. This means that larger parts of the acceleration has to be represented by tilt coordination.

Although tilt coordination is widely used in driving simulators it is a common opinion that it should be handled with care or even be avoided as far as possible, see e.g. [2, 3, 4, 5]. A too high tilt rate will be registered as rotation by the driver instead of as linear acceleration. Rate limiting of the tilt coordination will however give rise to time lag in the perceived accelerations [3]. This trade off between perceived rotation and time lag is further explained in Section 4.1.

1.2 Purpose

The purpose of this thesis is to investigate the possibilities to preposition the simulators x,y -sled to an off-centre starting point for upcoming accelerations and thereby virtually enlarge the motion envelope. That way a larger part of the accelerations can be represented by linear motion in the sled instead of by tilt coordination.

The scope is to, with the goal to improving the validity or realism and general driving experience, develop, implement and validate an additional prepositioning algorithm which will complement the currently deployed motion cueing algorithm in Sim IV. The developed prepositioning algorithm is described in Chapter 5.

1.3 Previous work

Chapron et al. [5] claim to use prepositioning in the SHERPA simulator, which has a similar configuration to Sim IV with a hexapod and an x,y -sled. The method is not described extensively but they hint of a similar approach to the one presented in this report. Chapron et al. concludes increased room for motion with prepositioning which allows for modified cut-off frequencies and the reduction of equivalent "acceleration deformation" and false cues. Weiß [6] presents a prepositioning algorithm with discrete offsets intended for use in the DLR driving simulator. Weiß was never able to test his algorithm in the real simulator and [5] was written before the SHERPA simulator was built. Thus neither papers have any results from experiments with test drivers.

1.4 Method

Initially a literature study was made in order to achieve a thorough understanding of the complex field of driving simulators in general and motion cueing in particular.

Two separate prepositioning algorithms were devised, one working in longitudinal direction and the other in lateral direction. The longitudinal prepositioning algorithm makes a prediction based on current vehicle velocity while the lateral depends on current vehicle velocity and upcoming road curvature.

The motion cueing algorithm used in Sim IV was written in Matlab Simulink [7] and is available in a desktop test environment. The prepositioning algorithm was implemented with separate subsystems in this environment and were tested and validated both separately and together with the motion cueing algorithm.

The prepositioning algorithm was tested and tuned on a desktop computer with

both test signals and vehicle model signals acquired from test runs in Sim IV. The results were also compared with simulation of the original, unaltered motion cueing algorithm.

The Simulink model was converted to C code which in turn was compiled to be executed in Sim IV. Initial test runs were performed with the motion system deactivated to ensure that the code was running properly. Pilot test runs were made with activated motion system and the prepositioning algorithm parameters are tuned.

A study was performed in order to validate the augmented driving simulator. Twelve test subjects, with varying driving experience and age, were asked to test drive the simulator twice and fill in a questionnaire. One of the drives were with, and the other without prepositioning. See Section 6.3.

1.5 Limitations

As the purpose of this thesis is to improve the current MCA with an additional prepositioning algorithm, no changes were made to the structure of the current MCA, except for parameters such as tuning of filter cut off frequencies.

Prepositioning is only made for motions that are presented in the x,y -sled, i.e. surge and sway motion.

Although the prepositioning algorithm can be modified to work with the simulator in truck mode, i.e. with the truck cabin and vehicle model instead of the ditto car, it is outside the scope of this thesis.

1.6 Main results

The prepositioning algorithm does enable more motion to be represented in the x,y -sled. An increase of 10 to 25% in the longitudinal acceleration and 21 to 53% in the lateral accelerations are represented in the sled in the tests. Results from the study also show that participants rank the test run with prepositioning on higher than the one with prepositioning off. The results are presented in Chapter 6.

2 Driving simulators

A large number of driving simulators of many different types exist or have existed throughout the world, see [8, 9]. They are used for many different purposes like training, research on driver behaviour, testing of new infrastructure, development of vehicle subsystems, and even for entertainment [8, 9, 10]. The benefits of using simulators instead of real vehicles in research are, apart from the obvious safety aspects, the possibility of strict control and repeatability of the driver environment [8, 9].

2.1 Simulator types

Because of the many different fields of application and the absence of construction standards, no two driving simulators are alike and each are to be considered a "prototype in itself" [9]. Despite that, one can easily identify two main categories, static or fixed-base and dynamic or motion-base driving simulators [11, 12, 13]. The dynamic driving simulators have motion systems allowing the driver to feel the vehicle movements. The earliest driving simulators were static with only some form of visual and auditory feedback [8, 9]. Technical advances and better understanding of psychological and psychophysiological effects have led to improvements in simulator validity and the addition of motion systems which are letting the driver experience accelerations [9].

2.2 Motion-base driving simulators

The motion of a mechanical system is often described by its degrees of freedom, DOF. Translational motion in the Cartesian x -, y - and z -axes are called surge, sway and heave respectively. Rotation around the x -, y - and z -axes are called roll, pitch and yaw. A simplified automobile with no suspension travelling on a flat road can be described as having three degrees of freedom, 3-DOF, i.e. surge, sway and yaw. Adding suspension and the possibility to travel up and down roads in the hills the automobile has six degrees of freedom, 6-DOF, translation along and rotation around the three axis, surge, sway, heave, roll, pitch and yaw.

One can simulate the motion of a vehicle in many ways and since there are no two driving simulators alike the number of different motion systems are almost as many as there are simulators. Despite the uniqueness of each simulator the seemingly most popular types of motion system today are based on so called hexapods or Gough-Stewart platforms [2, 8, 11, 14, 15]. The hexapod consists of a base with six linear hydraulic or electromechanical actuators connected to a moving platform capable of 6-DOF, see Figure 2.1. The drivers cabin is placed on top of the platform.

The hexapod is usually rather small and its motion envelope limited. To overcome this limitation some more advanced driving simulators, like the Sim IV, have the cabin and hexapod placed on top of a sled capable of large translational movements in one or two axis [2, 8]. See Figure 2.2. These simulators, although only really capable of six degrees of freedom are said to have 8-DOF [2] or (6+2)-DOF [9]. The hexapod also has the possibility to perform tilt coordination, which is described in Section 3.2.

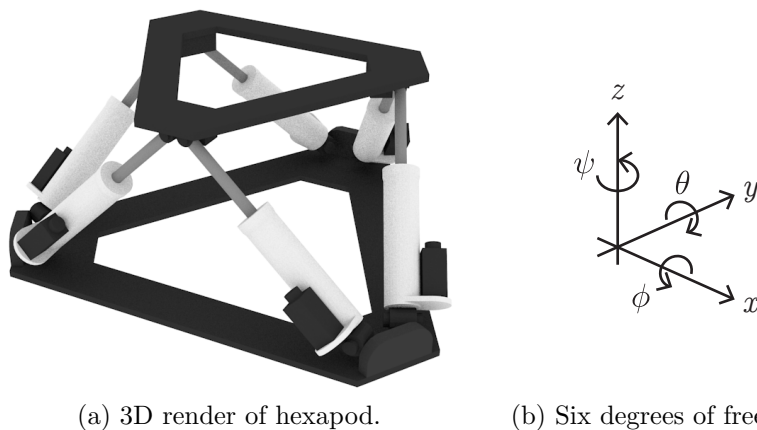


Figure 2.1: 3D sketch of a hexapod and its degrees of freedom.



Figure 2.2: 3D render of the full motion system.

3 Motion Cueing

As mentioned earlier, in order to improve the validity of a driving simulator a motion system which makes the driver experience the accelerations of the simulated vehicle can be used. Since every motion system have physical limits in their motion envelope it is usually not an option to recreate the simulated motions one-to-one. The way the signals from the simulated vehicle are filtered and then represented in the motion system is called a motion cueing algorithm, MCA. Depending on the available motion system, different approaches can be made. High frequent linear accelerations are, if possible, replicated by a corresponding translational movement in the motion system. Sustained, low frequency acceleration are difficult to represent due to the limits of the actuators and the available motion envelope. Instead such accelerations are represented by tilting the hexapod, tilt coordination.

3.1 Human motion sensing physiology

The body functions that give a human the sense of motion and orientation can be accredited to a number of different receptors throughout the body. These include visual input through the photoreceptors in the eyes, movement and posture via proprioceptors throughout the body and accelerations and orientation via the vestibular system [16]. When working with dynamic driving simulators it is the vestibular system, which is sensitive to acceleration, rotation and orientation in the gravitational field, that plays the most important role [8].

3.1.1 Vestibular system

The vestibular system is used to register translational and rotational acceleration as well as orientation of the body, or more precisely, the head. It is located in the inner ear and consists of two sets of sensory organs, the semi-circular canals and the otoliths [16]. There are three semicircular canals which, thanks to their perpendicular configuration, respond to angular velocity in roll, pitch and yaw. The two otoliths on the other hand register linear acceleration. Due to an ambiguity in the vestibular system there is no difference in perception of linear acceleration and gravitational acceleration resulting from tilting of the head [8]. This phenomena is utilised in motion cueing in tilt coordination, TC, which is described in Section 3.2. Both the semi-circular canals and the otoliths have what is called a perceptual threshold, a lower limit of the acceleration for the otoliths or rotational velocity for the semi-circular canals that can be sensed [17]. In the motion cueing context it is preferable to avoid cues below the threshold, since they can not be perceived. In the washout phase it is however the opposite, only low accelerations are desired. For the purpose of preposition it is crucial to stay below the perception threshold to avoid

rendering false cues, i.e. motion cues that are unprovoked and unexpected.

A study to find the threshold of linear acceleration detection was made by Benson et. al. [17]. The visual and auditory cues were however suppressed in the experiment and the test subjects were not only asked to signal the detection of motion but also the direction. The mean threshold for linear acceleration detection in the x -axis was found to be 0.063 m/s^2 and in y -axis 0.057 m/s^2 [17].

A corresponding study performed by Groen et al. [18], showed a threshold for rotational velocities at $3^\circ/\text{s}$. There is however another study by Nesti et al. [19] that indicates that when combined with visual cues as in a driving simulator rotational velocities up to $6.3^\circ/\text{s}$ go unnoticed.

3.2 Tilt Coordination

The human motion sensing organs, the vestibular system, described in Section 3.1, can not differentiate between translational and gravitational accelerations. Thus tilting the cabin around the drivers head and using a component of the gravitational vector will give rise to an acceleration in the drivers horizontal reference plane [8]. This in combination with (non-tilting) visual cues is perceived as a continuous translational acceleration [2, 8, 9, 20], see Figure 3.1. This practice must be performed under the perception threshold for rotation in order to avoid presenting false cues, motion sickness or other side effects. It is a common opinion that it should be handled with care or even be avoided as much as possible, i.e. only using it to represent low frequency linear accelerations [2, 3, 4, 5].

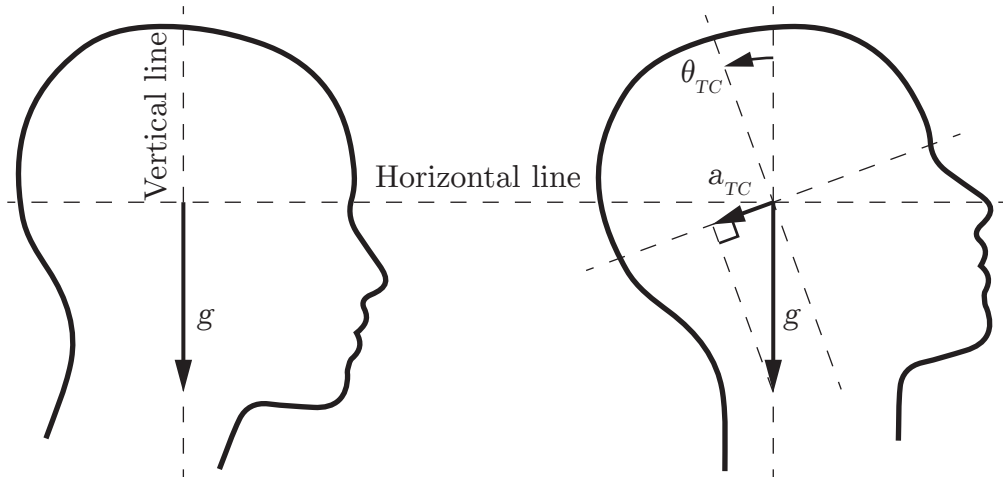


Figure 3.1: Tilt coordination principal sketch.

3.3 Washout filters

Most driving simulator still utilize some variant of what is called a washout filter. Depending on the available motion system this can be implemented in different ways. In principle it works by dividing the vehicle acceleration into three channels: translational, rotational and tilt coordination [20].

The high frequency part of the translational acceleration of the simulated vehicle is represented by translational movement in the motion system. The low frequency translational parts and high frequent rotational rate (in roll and pitch) are represented by angular movement of the motion system. This is achieved by filtering the acceleration signals from the simulated vehicle, a_{vh} , through high- and low-pass filters, see Figure 3.2. The desired angular rates, ω_{vh} , from the vehicle model are also high pass filtered to stay over to the human perception threshold. When implemented, the washout filters are generally modified with scaling and limiters etc. [21]. The washout filter is also responsible for returning the motion system to its neutral position, ideally through movements below the human perceptual threshold.

3.3.1 Classical washout algorithm

The classical algorithm was originally developed by Reid and Nahon [21] to be used in flight simulators, but was soon adopted into driving simulators where it is still the most commonly used algorithm [11]. The classical washout filter uses constant filter parameters on the high and low pass filters. It has a great appeal due to fairly straightforward implementation and is still widely used. One large disadvantage of this MCA is that the filters needs to be tuned for the worst case scenario in respect to acceleration magnitude and duration. The system must be tuned in such a way that the actuators boundaries are never surpassed. Since normal driving operations are generally far below the worst case, this strategy can result in a poor utilisation of the available motion envelope [22].

3.3.2 Adaptive washout filter

In a way to overcome the disadvantage of the classical algorithm the so called "adaptive algorithm" was devised [23]. In this approach the parameters of the filters are not kept constant. Instead they are at each time step calculated by minimising a cost function. By not using fixed parameters in the filter a larger part of the motion envelope can be utilised while still not exceeding the motion systems boundaries. This means that manoeuvres that use substantial motion cues, like braking, are filtered more heavily than more modest manoeuvres. A disadvantage to this approach is the fact that motion of different intensity in the simulated vehicle are rendered the same by the motion system [8].

3.3.3 Optimal washout filter

Another approach with some similarities to the adaptive algorithm is the so called optimal algorithm. The optimal algorithm also seek to minimise a cost function to find the optimal filter parameters at any given time. But unlike the adaptive algorithm the optimal filter also take the drivers perceptual system into account. As developed in [24] an optimisation criterion based on the difference between the output from the simulated model and the motion system filtered through a model of the human vestibular system. Since it has a rather high complexity and the difficulty in obtaining a good model of human perception, no real implementation of this algorithm has been done [8].

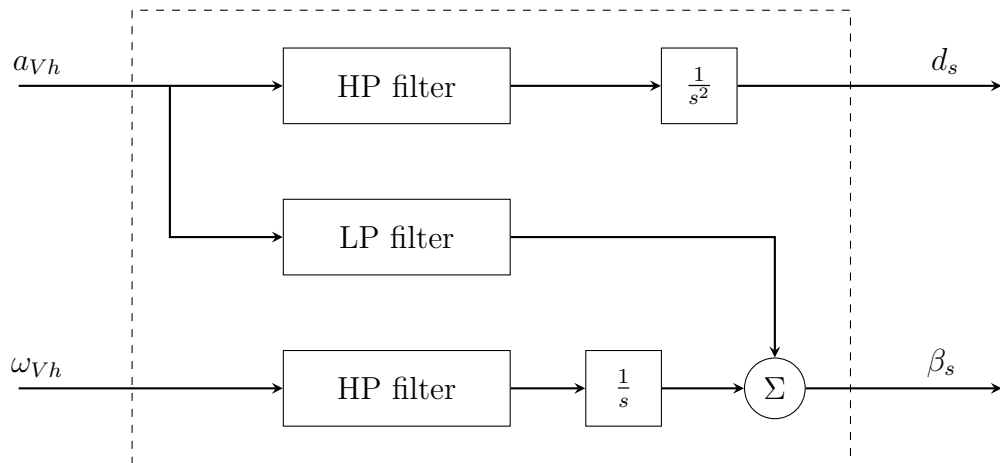


Figure 3.2: Principal block diagram of a washout filter.

4 Sim IV

The driving simulator used in this project is as mentioned VTI's Sim IV. It is a dynamic driving simulator consisting of a driver's cabin enveloped by a dome placed upon a motion system, see Figure 4.1. More images of Sim IV are available in Appendix G. It is possible to switch between either a truck cabin or the front half of a passenger car. The visual cues are provided by eight fish eye LCD projectors placed inside the dome giving the driver a 210 ° field of view. The visual system also include three LCD screens as side and rear view mirrors. The motion system of Sim IV is a 8-DOF system, described in Section 2.2, it consists of a large hexapod which in turn is mounted on top of an x,y -sled. The hexapod has a fairly limited displacement compared to the sled but can, thanks to its faster dynamics, represent motion of higher frequencies than the sled. The maximum linear displacements of the motion systems can be seen in Table 4.1.

Table 4.1: Maximum displacements of Sim IV [25]

	Surge [m]	Sway [m]	Heave [m]
Hexapod	± 0.31	± 0.31	-0.240/+0.261
Sled	± 2.500	± 2.295	-

4.1 Motion Cueing in Sim IV

The motion cueing algorithm used in Sim IV is a variant of the classical washout algorithm, see Section 3.3.1, which is a system of filters that divide the vehicle accel-



Figure 4.1: The VTI Sim IV driving simulator, dome and motion system.

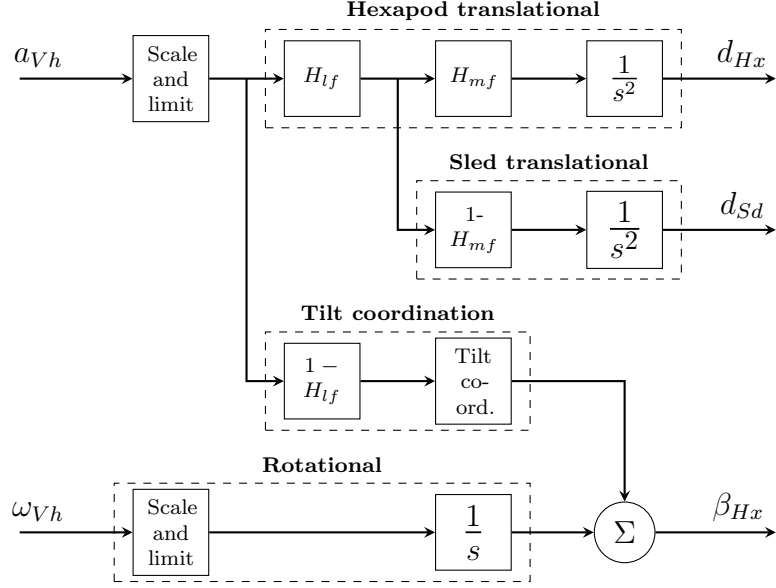


Figure 4.2: Principal block diagram of the motion cueing algorithm used in Sim IV. Figure recreated from [3].

erations between normal translations and tilt coordination. The classical algorithm as depicted in Figure 3.2 was originally developed for use in 6-DOF motion systems, i.e only a hexapod. In the Sim IV MCA there is an additional frequency splitting of the accelerations in the surge and sway directions, the middle frequencies are passed to the x - y -sled. There is also a lane dependant algorithm incorporated in the sway direction which takes the current lane position into consideration. A simplified version of the motion cueing algorithm used in the lateral and longitudinal directions can be seen in Figure 4.2 (lane dependant algorithm not included).

The inputs to the system, the translational accelerations a_{Vh} and rotational velocities ω_{Vh} of the simulated vehicle, are first scaled and limited in order to keep the motion system within its physical boundaries. The angular velocities can only be represented by the hexapod and are simply scaled, limited and integrated to obtain the desired angles β_{Hx} . The translational accelerations are divided into high-, middle- and low frequency components. The low frequency parts are separated by the high pass filter H_{lf} and its complimentary filter $1 - H_{lf}$, both with cut-off frequency ω_{lf} . The high frequency part then undergo the similar treatment again by the complementary filters H_{mf} and $1 - H_{mf}$, with cut-off frequency ω_{mf} . The high- and middle frequency signals are then integrated twice and passed to the hexapod and sled respectively as position signals. The low frequency part is passed to the tilt coordination and added to the angles β_{Hx} .

It is common to use tilt rate limiting on the tilt coordination in motion cueing since rotating above the human perceptual threshold for angular velocities, which is about $3^\circ/\text{s}$ [18], can lead to false cues. Introducing a rate limit on the angular velocity will however come with the drawback of a time lag in the perceived acceleration. In a study performed by Fischer et al.[3] a conclusion is drawn that time lag has a greater

negative effect than false cues due to fast tilting on the validity of the motion. There are also studies that indicate that the perceptual threshold for angular velocity is higher when combined with visual cues that contradict the rotation, as is the case in a driving simulator [19]. In light of this a trade off is made using a rate limit which is above the perceptual threshold but will generate a lower time lag.

The motion cueing system can be tuned by adjusting the scaling, limits and cut-off frequencies of the filters. There is also the washout filter itself, which is not depicted in Figure 4.2 for clarity, which also has tunable cut off frequencies that influence the performance of the system. The tuning of a motion cueing system can be difficult and arduous since few objective validation methods exist. The system needs to be validated by human perception, i.e. test with humans have to be made.

5 Prepositioning

As mentioned in Chapter 3, the overall problem to be dealt with in motion cueing is the difficulty of reproducing large vehicular movement in the limited work space of the simulators motion system. In general it is advised to avoid tilt coordination as far as possible [2, 3, 4, 5]. By predicting which motions that are likely to occur, e.g. acceleration, braking, turning etc., one can preposition the motion system accordingly and thus enabling the ability to represent a larger part of the simulated vehicles movements in the sled. For driving simulators this is of interest primarily for movements in the surge, sway or yaw directions since road vehicles generally only experience limited movement in the heave, roll and pitch directions. The motion cueing system then need to take the extra available space into account to be able to generate a larger movement in this direction.

The area of prepositioning in motion cueing is still not exploited in any great extent, a literature survey shows that only a few attempts have been made at implementing such functionality. The SHERPA simulator, developed by PSA-Peugeot-Citroën, has a prepositioning algorithm which preposition based on speed of the vehicle for longitudinal prepositioning and road database information for lateral prepositioning [5]. Another proposed prepositioning algorithm is suggested by Cornelius Weiß [6] and is intended for use in the DLR driving simulator. Weiß takes a quite complex approach and presents an algorithm which switches between different states depending on what type of preposition is desired. Both the above mentioned approaches aim to use their prepositioning algorithm as an extension of the classical washout algorithm, see Section 3.3.1. Both these sources only provide a quite rudimentary explanation on how the actual prediction part of the prepositioning is done, and none seems to have tested their solutions in a real simulator.

As mentioned earlier, a vehicle primarily moves in the surge, sway and yaw direction and thus it is in these directions prepositioning is of interest. The hexapod of Sim IV can represent movements in all these directions but with fairly limited stroke. Therefore all the prepositioning is done by the x,y -sled. The most significant movements that needs to be represented by the motion system is acceleration, braking and turning. Since acceleration and braking generally generate movements along the vehicles x-axis and turning along the y-axis it is natural to divide the cases into two algorithms, one for lateral and one for longitudinal movements. The lateral prepositioning depends on both the curvature of the road and the current vehicle velocity and will be referred to as road dependent prepositioning while the longitudinal will be referred to as velocity dependent prepositioning. Both these algorithms can be divided into three tasks:

1. Predict future events, i.e. upcoming curves, braking, etc.
2. Find the desired position of the platform to best represent the predicted event.
3. Move to the desired position, before the event occurs, without the driver

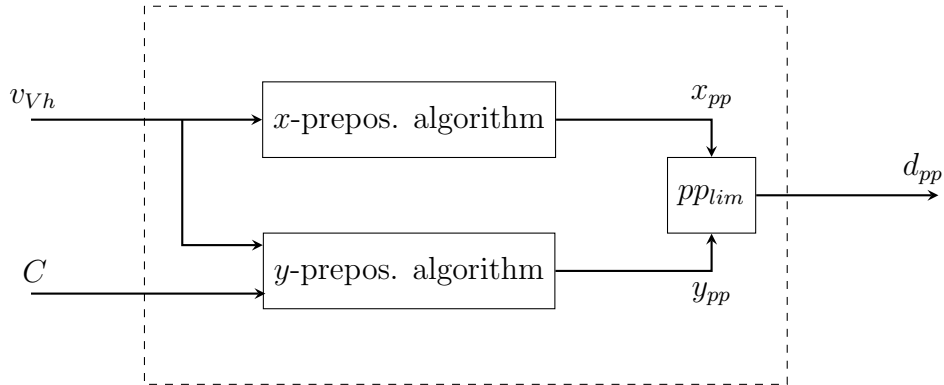


Figure 5.1: Principal block diagram of prepositioning subalgorithm.

noticing.

The first two tasks differ quite much in the lateral versus the longitudinal case and needs to be addressed in different manners while the third task is common for the two different cases.

Figure 5.1 shows a general block diagram of the prepositioning algorithm. It is made up of three subsystems addressing the above tasks: Predict and calculate the longitudinal and lateral prepositioning, and an acceleration limiter to keep the prepositioning motion under the human perception threshold, see Section 5.3.

5.1 Velocity dependent, longitudinal prepositioning

To make room for longitudinal accelerations, i.e. increasing speed and braking, the velocity of the vehicle is used for prepositioning. A normal, fully functional car or truck has higher braking acceleration performance than speed increasing, which is also the case for the vehicle models used in Sim IV.

The simulator needs to be prepositioned to prepare for any driver action. In general this means prepositioning the simulator at a point on the x -axis from which the driver can either increase speed or brake without hitting the motion system boundaries.

5.1.1 Vehicle model

Finding the longitudinal preposition requires knowledge about the vehicle model. There are a number of different models used in Sim IV. Assuming that they feature similar performance, the model chosen to be used to design the generic prepositioning algorithm was created by Jorge Gomez Fernandez [26] and is written in Modelica. It is based on a Saab 93 with a petrol engine and has simple drive line features where

the engines maximum torque is described by a polynomial. To find the optimal position one must know what maximum accelerations the vehicle can produce at different velocities and gears. The maximum engine torque is described in [26] as a polynomial on the form:

$$T_{e,max} = c_1\omega_e^3 + c_2\omega_e^2 + c_3\omega_e \quad (5.1)$$

where $T_{e,max}$ is the maximum torque from the engine and ω_e is the engine rotational velocity.

The gearbox has five gears with gear ratios g_i , $i = 1, 2, \dots, 5$, a fixed gear g_f and an efficiency η . Applying these ratios to both the torque and the engine rotational velocity gives the torque and rotational velocity at the driving wheels. The nominal wheel radius r_{nom} and the vehicle mass m_{Vh} gives the corresponding vehicle acceleration, Equation 5.2 and tangent velocity of the wheels which can also be interpreted as the velocity of the vehicle if there is no slip on the road, Equation 5.3.

$$a_{Vh,max} = \frac{T_{e,max}\eta g_i g_f}{r_{nom} m_{Vh}}, \quad (5.2)$$

$$v_{Vh} = \frac{\omega_e r_{nom}}{g_i g_f}. \quad (5.3)$$

Figure 5.2a shows the maximum acceleration curves for the five different gears as a function of the vehicle velocity converted to km/h.

The prepositioning in the x -axis is designed for the worst case scenario, i.e. the maximum possible accelerations at different vehicle velocities. A function based on the maximum values of the different gear settings are selected. The function is created with the Curve Fitting tool in Matlab and is on the form:

$$a_{a,max} = 51.84v_{Vh}^{-1}.$$

Since the function goes to infinity when velocity goes to zero it is subjected to a saturation at about 6 m/s², which is the maximum acceleration of the vehicle. The obtained curve is plotted in Figure 5.2b on top of the accelerations curves for clarification.

The maximum braking acceleration of the vehicle is constant, $a_{b,max} = 5$ m/s² at every vehicle velocity.

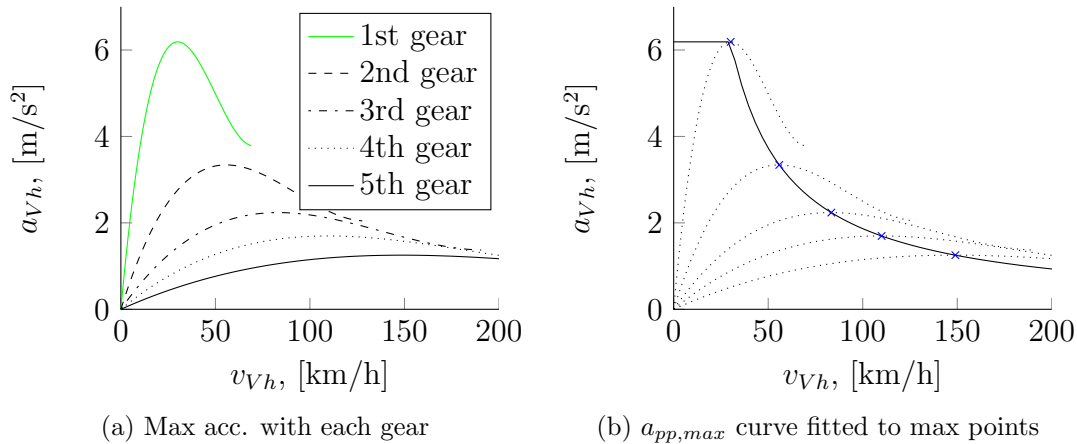


Figure 5.2: Vehicle acceleration model

5.1.2 Longitudinal prepositioning algorithm

An algorithm is devised that use the obtained maximum acceleration curve together with the maximum braking acceleration to formulate an optimal longitudinal preposition. The general idea is to, at any given vehicle velocity, calculate a possible maximum and minimum acceleration of the vehicle. By using this possible accelerations one can generate an optimal sled position enabling such large motion as possible without risking to hit the boundaries. A block diagram representation of the algorithm can be seen in Figure 5.3.

The first step is to calculate the maximum possible positive acceleration, $a_{a,max}$ of the vehicle based on the current velocity of the vehicle $v_{Vh,x}$ using the velocity/acceleration curve obtained in section 5.1.1. Since the possible acceleration, $a_{a,max}$, should correspond to the actual vehicle acceleration it is scaled and limited in the same manner as in the motion cueing algorithm, see Section 3.3.1. As the minimum acceleration, i.e. maximum braking $a_{b,max}$, is constant and not dependent on velocity it is simply limited like in the original motion cueing system.

Since it is not really possible to predict if an acceleration or braking is to occur, because of the non-deterministic human nature, one needs to take both possibilities into account in order not to hit any boundaries in the motion system. By calculating a mean value

$$\bar{a}(a_{a,max}) = \frac{a_{a,max} + a_{b,max}}{2} \quad (5.4)$$

one gets the curve depicted in Figure 5.4. As one would expect there is a larger positive acceleration at low speeds which decreases with increasing velocity.

This \bar{a} is then used to calculate a value x_{pp} by the function

$$x_{pp}(v_{Vh}) = \bar{a} \frac{x_{pp,max}}{\max(\bar{a}(a_{a,max}), |\bar{a}(a_{a,min})|)}. \quad (5.5)$$

This will for every velocity v_{Vh} generate an longitudinal preposition value in the span $[x_{pp,min}, x_{pp,max}]$. This value is then subjected to acceleration limiting to keep the

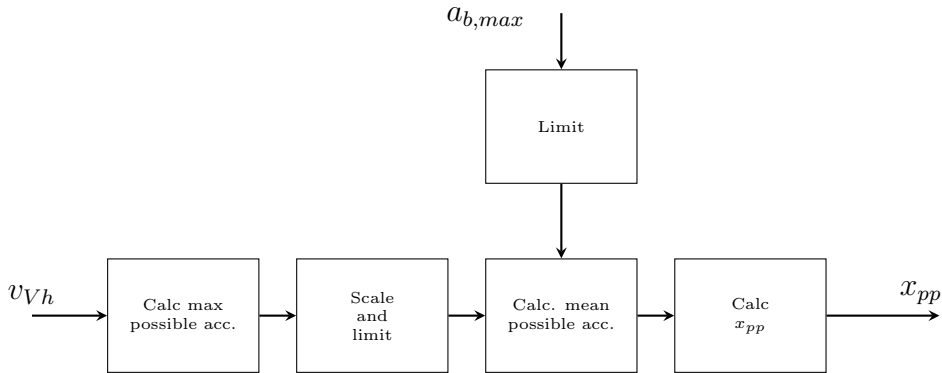


Figure 5.3: Principal block diagram of the longitudinal prepositioning algorithm.

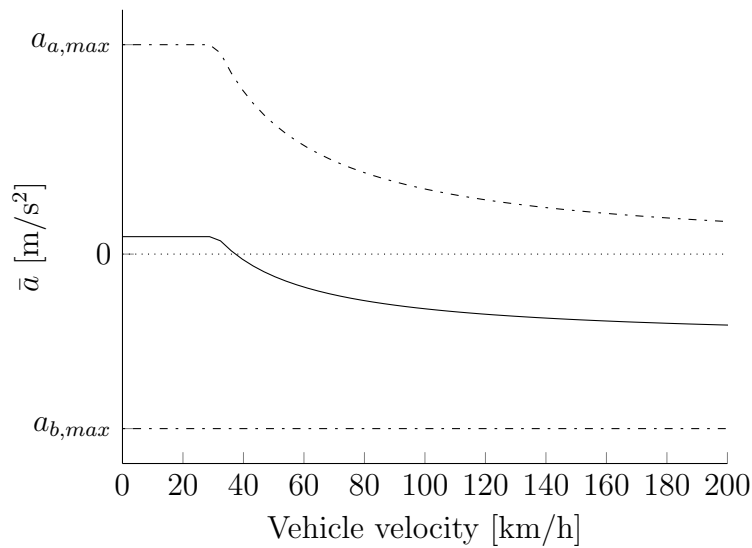


Figure 5.4: Mean possible longitudinal acceleration curve.

motion below the human perceptual threshold before it is passed on to the motion system.

5.2 Road and velocity dependent, lateral prepositioning

The simulated roads in Sim IV are described in an OpenDRIVE database, an open file format for the logical description of road networks [27]. It contains geometric information of the road such as lengths of road sections, number of lanes, curvature, junctions etc. The road is based on a reference line which is represented in OpenDRIVE as either a straight line, an Euler spiral, an arc or, less frequent, as a third degree polynomial [28]. An Euler spiral is in this case a curve with a linearly increasing or decreasing curvature whilst an arc is a curve with constant curvature, a circle segment. The reason why Euler spirals are used in curves is to

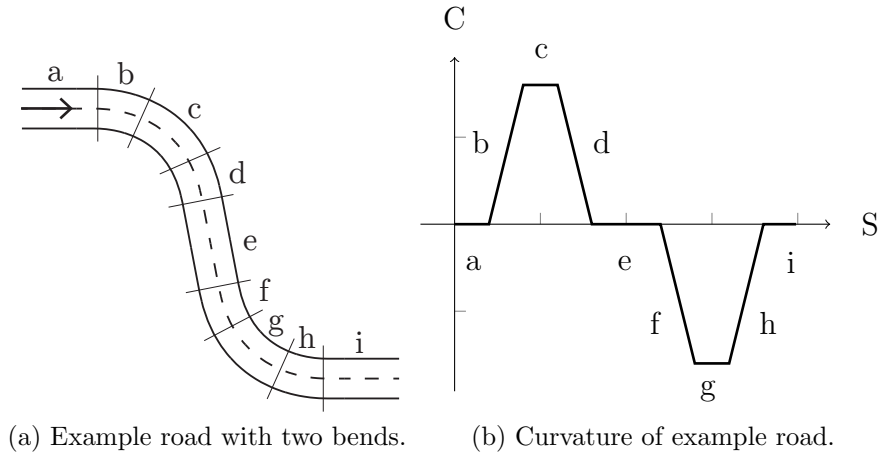


Figure 5.5: Example of road curvature.

avoid discontinuities in the curvature that would require the driver to change steering angle sharply to stay on the road. This usage of Euler spiral originates from the time of train development when increased velocity required smooth transitions between a straight and a circular arc curve [29].

An illustrative example road with two curves, one to the right and the one to the left can be seen in Figure 5.5a. The road has three straights (a, e and i). The two curves begins and ends with an Euler spiral (b, d, f and h) have constant curvature parts in the middle (c and g), i.e. circular arcs. Figure 5.5b illustrates the curvature C of the example road as a function of distance on the road S . Right curvatures are positive, left are negative.

5.2.1 Data collection

The road data is geometrically defined which means that the computer running the road simulation can also make calculations based on these data. E.g. one can request the curvature at any specific point on the road. The road dependent prepositioning is calculated based on this kind of data. To predict future lateral movements the curvature is collected via a function in the OpenDRIVE library. The curvature is sampled at a specific time t_h in front of the car which results in different curvature frequencies depending on the velocity of the car.

The lateral acceleration a_n of a point mass in a curve with radius R , see Figure 5.6, is

$$a_n = R\omega^2, \quad (5.6)$$

where ω is the angular velocity and the curvature C is the inverse of the radius R

$$C = \frac{1}{R}. \quad (5.7)$$

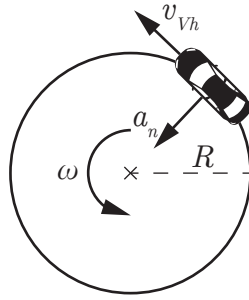


Figure 5.6: Principle sketch of lateral acceleration in curves

The angular velocity can be written as

$$\omega = \frac{v_s}{R}. \quad (5.8)$$

Combining Equations 5.6, 5.7 and 5.8 we get an expression of the lateral acceleration a_n as a function of the curvature C and the velocity v_s

$$a_n = C v_s^2. \quad (5.9)$$

5.2.2 Lateral prepositioning algorithm

As described in the previous section one can easily calculate a lateral acceleration a_n in a curve with curvature C depending on the velocity v_s . If one can make these calculations based on an upcoming curvature it is also possible to make a prediction of future accelerations.

A schematic of the lateral prepositioning algorithm can be seen in Figure 5.7. The inputs to the system are the current longitudinal velocity of the vehicle, $v_{Vh,x}$, which is assumed to be constant, and the curvature C at a time t_h in front of the vehicle. First the upcoming lateral acceleration is calculated based on upcoming curves and the current velocity. In order to predict an actual motion to be represented in the motion system the predicted upcoming acceleration is subjected to the same scaling and limiting as is done in the motion cueing algorithm, see Section 3.3.1. Since the prepositioning algorithm is limited to motion in the sled it uses the same filter used to split the accelerations by frequency in the MCA, letting through only the middle frequency parts of the signal. This ensures that prepositioning is done only for accelerations that will be represented by the sled.

The obtained predicted accelerations are then integrated twice to achieve a position signal and are then subjected to a saturation which limits the signal to not exceed $\pm y_{pp,max}$, which is the maximum preposition displacement, see Figure 5.15.

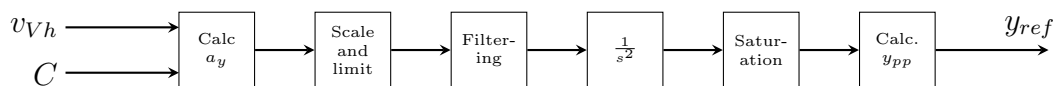


Figure 5.7: Principal block diagram of the lateral prepositioning algorithm.

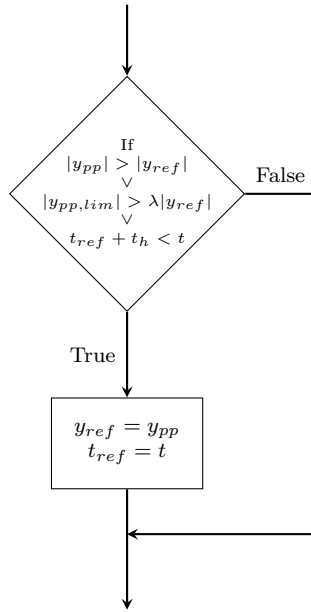


Figure 5.8: Principal logic block.

It is desirable to always preposition the system according to the maximum acceleration predicted within the given time horizon t_h . t_h is chosen as the time it takes to move the sled to a preposition in a worst case scenario. This implies that one can not simply take the signal y_{pp} calculated above as a reference. In every simulation step the current calculated y_{pp} is checked against the highest value within the prediction horizon, y_{ref} . y_{ref} is also checked against the acceleration limited current output of the prepositioning system to see if the reference is reached. Thirdly the time of which the reference displacement should occur, t_{ref} is within the prediction horizon and not has passed. If any of these three conditions are fulfilled y_{ref} and t_{ref} are updated according to

$$y_{ref} = y_{pp} \text{ and } t_{ref} = t.$$

A block representation of the logic can be seen in Figure 5.8.

A calculation of y_{ref} based on the curvature of parts of the test road visualised in Figure 5.5, can be seen in Figure 5.9. In this example a prediction horizon t_h of 7.5 s is used and the prepositioning is limited at $\pm 1m$. Both these are tunable parameters in the model and can be altered based on application. Calculations are made at a constant longitudinal vehicle velocity of 15 m/s.

As seen in Figure 5.9 the system calculates a positive preposition for the onset of the curve at time 20 s. Only the onset, i.e. the start of the acceleration is represented by the sled, the rest of the sustained acceleration is represented by tilt coordination. There is a negative preposition to prepare for the curvature changes at time 40 s and 50 s. Although there is no actual negative acceleration of the vehicle the acceleration in the sled must be negative in order to compensate for the slowly changing sustained accelerations represented by tilt coordination. After around time 55 s a positive desired prepositioning is seen although there is no upcoming curvature. This undesired prepositioning is a result of how the signal, i.e. the predicted lateral

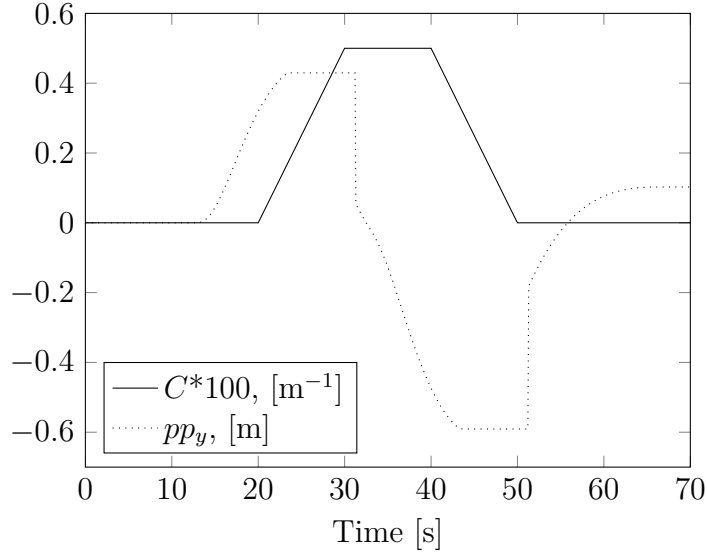


Figure 5.9: Test road curvature, (C) and road dependent, lateral prepositioning, (pp_y)

acceleration, is processed by the motion cueing algorithm. After being filtered through the frequency splitting filter, a high pass filter, and thereafter the washout filter, which is also a high pass filter, a slight overshoot can be observed when the signal returns to zero. Since the prepositioning is calculated based on the maximum acceleration in the current time horizon the prepositioning after time 60 s is based on the peak overshoot.

5.3 Acceleration and jerk limitation

As mentioned in the beginning of this chapter, the third task of the prepositioning algorithm is to make the x,y -sled reach the desired preposition before the intended acceleration is to be represented, without the driver sensing the motion. Moving the drivers cabin without the driver noticing is a challenge that requires knowledge about the human physiology and motion perception. As described in Section 3.1 the horizontal linear acceleration perception threshold of a human lies around $0.05 m/s^2$, [17]. Some authors also believe that jerk, the derivative of acceleration, has effects on both the perceived strength of motion and linear acceleration detection thresholds [4, 30]. The detection threshold figures presented by [17] are therefore to be considered sensitive to combinations of acceleration and jerk although there are no figures on the jerk limits available. The unarguably optimal way to reach the desired preposition with initial- and target velocity of zero is to maximize the acceleration and jerk for half the distance and then invert to brake the rest of the distance. A bang-bang solution to a minimum time problem with limited acceleration and jerk.

The current motion cueing algorithm has a non-linear limiter that make use of Hermite polynomials [31] to slow down the sled when it reaches its boundaries. It

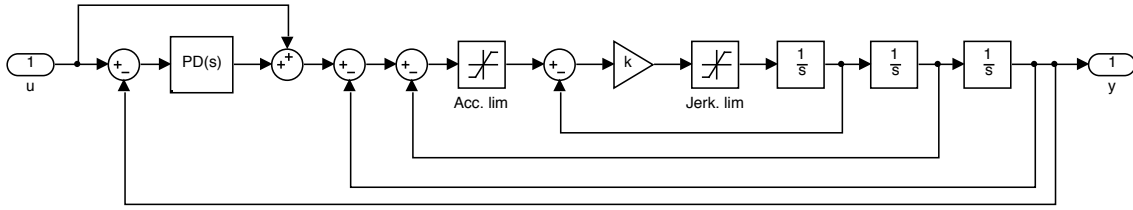


Figure 5.10: Principal block diagram of the acceleration and jerk limiter.

works as a smooth saturation of the position but does not give full control of the maximum first and second derivative of the displacement [32]. For the purpose of improving the motion of the simulator the MCA is prepared with a "Jerk Limiter" subsystem [31] which has the ability to control not only jerk but also acceleration and velocity. It is currently not used since it applies a delay in the direct motions which have more negative effects on the validity than it has benefits [1]. Small delays are however not a big issue when it comes to repositioning since it refers to non-perceivable motions. Therefore the acceleration limiter implemented for the repositioning algorithm is an adaptation of this jerk limiter. As described in [32] the displacement, in this case the position of the x,y -sled, is differentiated, saturated to the required level and then integrated again. This however introduces two non-linearities, the saturations, which in turn introduce sustained oscillations. Fischer [32] referring to the work of Hippe [33] uses PD controllers in combination with a feed forward loop to control the signal. A block diagram of the acceleration limiter is presented in Figure 5.10.

The maximum allowed acceleration in each direction is denoted a_{lim} and the maximum jerk j_{lim} . Since j_{lim} as opposed to a_{lim} can not be set to a scientifically motivated number, it has to be empirically studied. This is described in Section 6.2.

Repositioning will often take place in both longitudinal and lateral direction. Maximising, in a worst case scenario, the acceleration and jerk in both axes will result in total higher levels than allowed, see Figure 5.11, $a_{pp,tot} > a_{lim}$. Benson et al. [17] does not mention the possibility that the vestibular system receive acceleration cues in two axes simultaneously. It is assumed that if the vestibular system is sensitive to combinations of accelerations, the small difference in maximum acceleration is negligible. Each repositioning axis will be limited by the acceleration and jerk limiter individually.

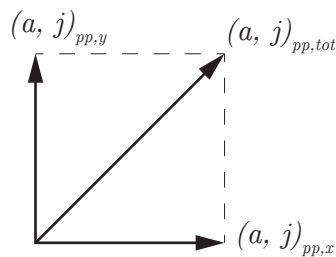


Figure 5.11: Acceleration resultant.

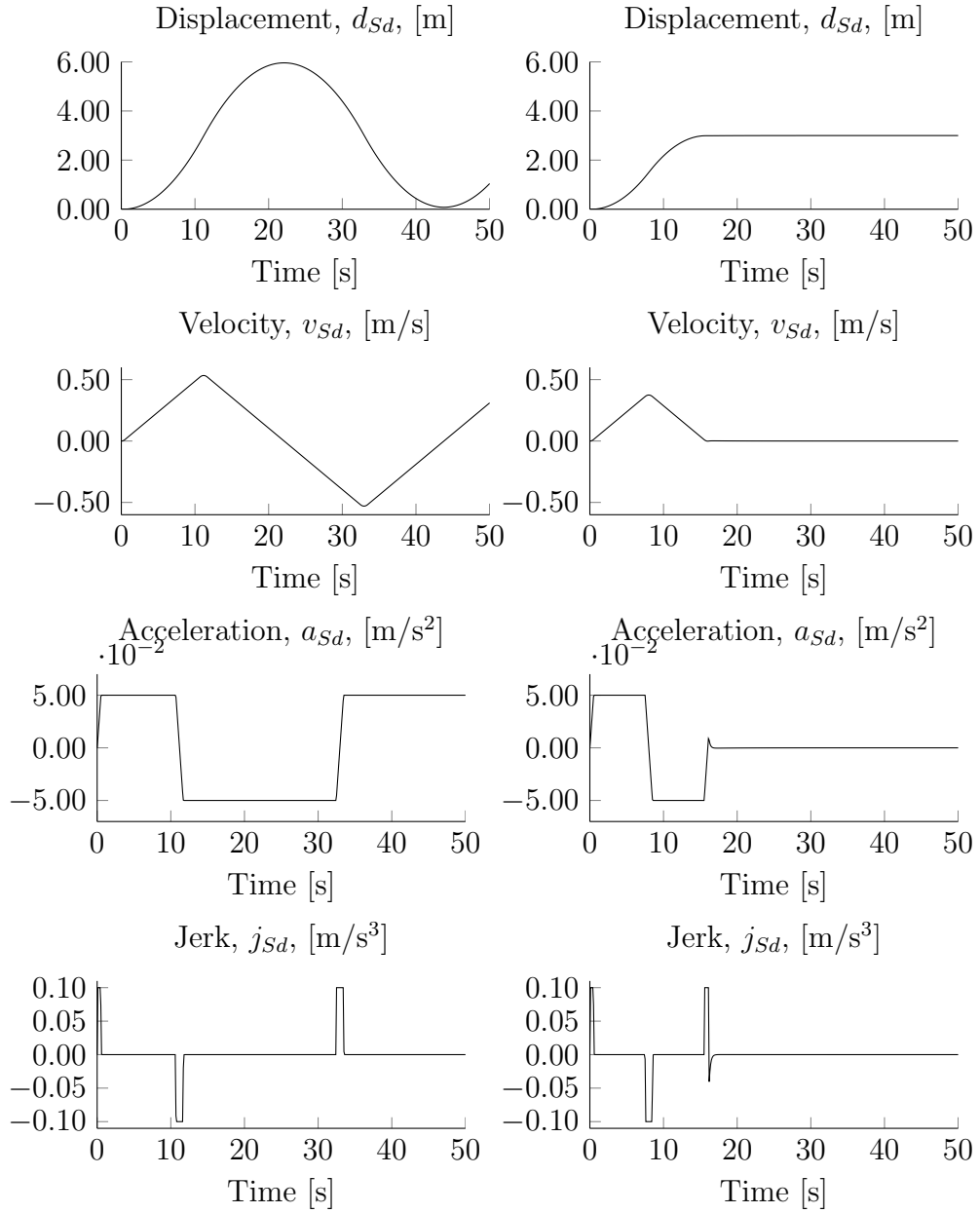


Figure 5.12: Step response of saturated acceleration and jerk without controller (left) and with controller (right).

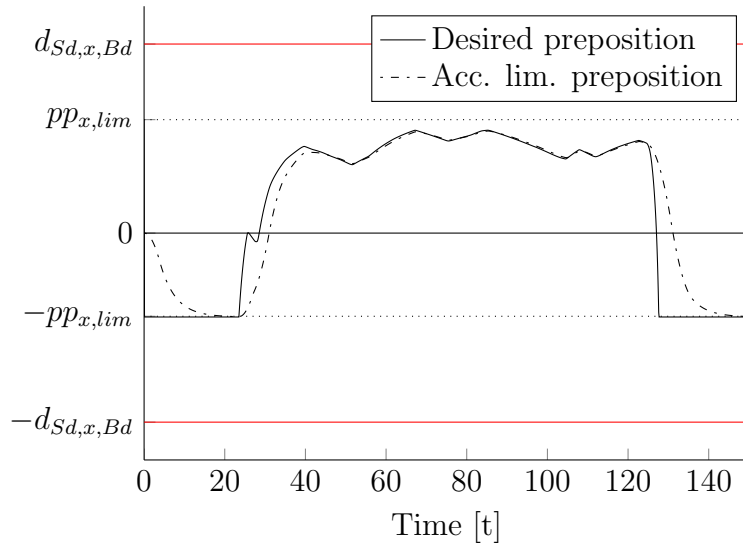


Figure 5.13: Longitudinal prepositioning in real test drive signal.

The maximum prepositioning acceleration is set to $a_{lim} = 0.05 \text{ m/s}^2$ which is below the human horizontal perception threshold. The PD controller is tuned for an optimal positioning of a maximum prepositioning step of 3 m, which represents a motion from one boundary to the opposite in the prepositioning motion envelope. The prepositioning algorithm and acceleration limiter settings can be found in Appendix D. Figure 5.12 shows the step response of the acceleration and jerk limiter with and without PD controller.

In Figure 5.13 one can see the calculated desired longitudinal preposition together with the actual, acceleration limited preposition. The calculation is based on a real test drive in the simulator. It shows a delay in the acceleration limited signal but it still manage to follow the reference quite fast.

5.4 Expanding the motion envelope

When a suitable preposition is achieved one has to be able to use the extra space made available. The currently used motion cueing algorithm does not really take available space into account, if nothing is done to enlarge the possible motion envelope there will be no difference in the perceivable motion of the system. One can take different approaches to this; in the scope of the current motion cueing system there are three different factors which can be changed in order to generate larger motion, altering the scaling factors of the accelerations, changing the limits or changing the cut off frequencies of the motion cueing filters or a combination of the three.

Changing the scaling factors is a pretty straightforward approach. It is easy to see that using a larger scaling factor generates a larger motion in the sled. A drawback is however that this only increase the energy in the sled. This implies that the on-set

of the acceleration, the high frequency part of the accelerations which is presented by translational movements in the hexapod, is lower than what is represented by the sled. I.e. the driver will experience a sudden jump in acceleration when the sled take over. Changing the limits of the system will produce a similar result although it is a blunter tool since it will only influence the high amplitude parts of the accelerations.

A better solution is to alter the cut-off frequencies of the frequency splitting filter used in the classical washout algorithm. As discussed earlier, the use of tilt coordination should be avoided as long as possible. It is therefore of primary interest to transfer energy from the low frequency parts, i.e. the accelerations represented by tilt coordination, to the middle frequency part and represent it in the sled. With this approach the tilt coordination part of the accelerations will set in later and there are good chances of reducing or in part eliminating the false cues generated by tilt rates above the perception threshold. The human perceptual threshold for angular velocities is around $3^\circ/\text{s}$ [18].

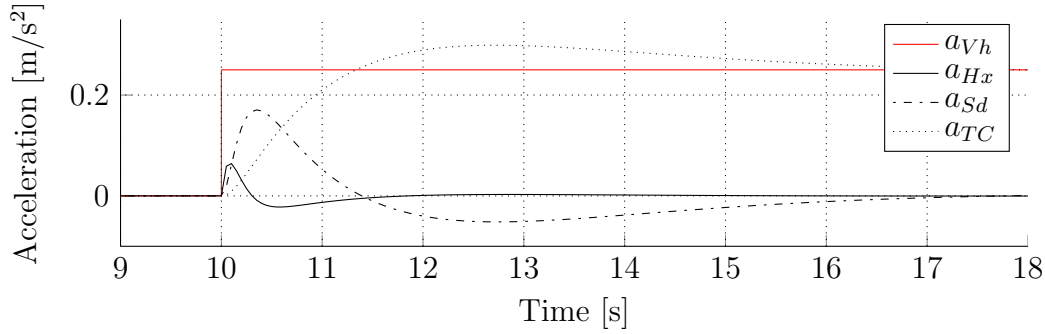
In practice this means altering the parameter ω_{lf} which is the cut off frequency of the high pass filter H_{lf} used in the frequency splitting part of the motion cueing algorithm described in Chapter 3 and Section 4.1. Figure 5.14 show a step response of the motion cueing algorithm with two different values of ω_{lf} . It is obvious from these plots that a lower value of ω_{lf} as in Figure 5.14b result in larger part of the accelerations being represented in the sled, a_{sd} in the figure, and the tilt coordination, a_{TC} builds up slower, compared with Figure 5.14a. By these plot one can also make the deduction that a slower build up of acceleration passed to tilt coordination will also result in a lower rotational velocity due to tilt coordination.

There are two different possible ways to altering the cut off frequencies in question, one can either statically alter the parameter or make the parameter time-variant, i.e. changing it on-line based on some criterion. The later approach is discussed in Chapter 7. In the repositioning algorithm the cut off frequencies are static. These parameters however need to be tuned in the actual simulator to ensure that the boundaries are respected.

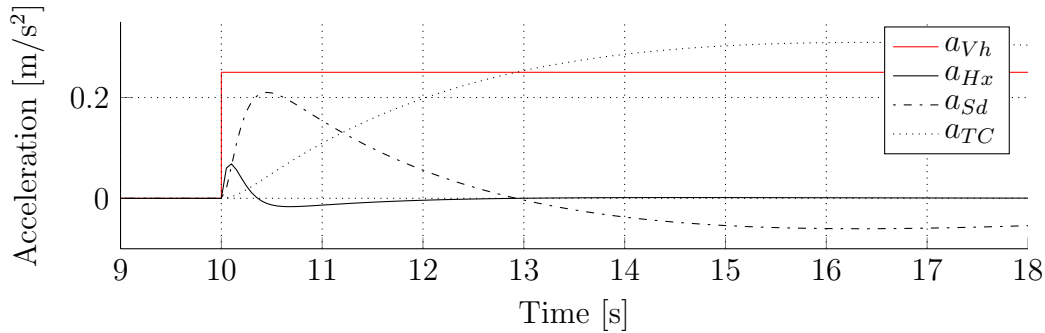
The boundaries of the repositioning motion envelope is set to $x_{pp,min}$, $x_{pp,max}$ and $\pm y_{y,max}$ to make room for unexpected manoeuvres, see Figure 5.15.

5.5 Implementation

The current motion cueing algorithm was developed in Matlab Simulink [7], a block diagram based simulation tool. The model is used to generate C code that is compiled and used in the actual simulator computers. The Matlab Simulink environment makes it easy to generate and test different subsystem to the motion cueing algorithm. Since it has not been in the scope of the project to alter the currently used motion cueing algorithm the repositioning has been developed as a separate subsystem block which can easily be enabled or disabled. The lateral and longitudinal repositioning



(a) Frequency splitting of acceleration, high ω_{lf} .



(b) Frequency splitting of acceleration, low ω_{lf} .

Figure 5.14: Comparison of frequency splitted acceleration with different ω_{lf} .

and acceleration and jerk limiter are also placed into three separate subsystem blocks and can be used individually.

Since it is practical to be able to simulate the motion cueing algorithm off-line, i.e. without having to run it in the actual simulator there is a test-suite available where one can use pre-recorded signals from the vehicle models as inputs or use generic test signals as steps, ramps etc. This enables the possibility to concurrently test and verify each step of the developed models.

5.6 Safety

Since the Sim IV motion system is built around powerful actuators capable of tossing both a human and half a car or truck cabin about, safety is of utmost importance. Besides the established safety routines practised on VTI when running the simulator, care has to be taken when modifying the motion software. The current MCA is tuned to scale down and limit motions so that the simulator always stays well within its physical boundaries. Since the parameters that control how much energy represented in the hexapod and x,y -sled are changed with the prepositioning, there is a risk that the sled in some situations move dangerously close to or even hit its boundaries. The MCA has software boundaries in the sled which are utilised with non-linear

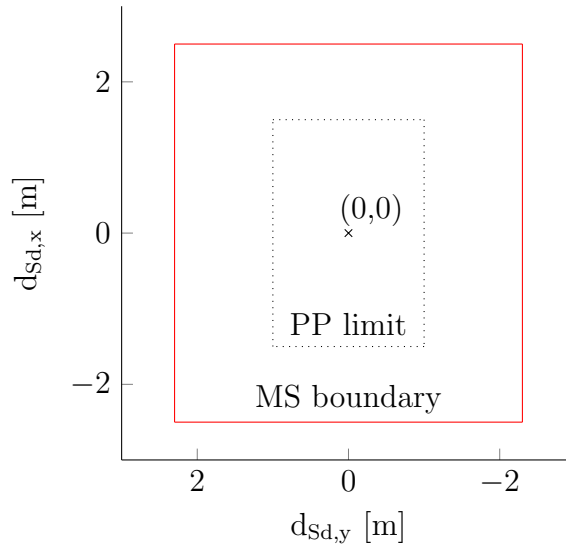


Figure 5.15: Top view of sled boundaries

limiter Hermite polynoms [31] which slows down the sled. This safety feature is intact and un-bypassed when the prepositioning algorithm is active. Even though simulations have shown that both boundaries and other limits specified by the motion system manufacturer are respected, initial tests was performed carefully at low speed. Additionally the motion system hardware have cushioning areas at the actuator stroke ends as a sort of last resort [31].

All sharp test runs in the simulator, with motion, are performed under the supervision of VTI simulator personnel.

6 Results

The validity of a driving simulator is as mentioned difficult to ensure by objective methods. Subjective test with human subjects are often necessary. There are however some criterion which can be assessed by objective tests:

- Use tilt coordination as little as possible.
- Keep the tilt rate as low as possible, preferable below the human perceptual threshold.

The results are presented in three parts, the first treat simulation results, i.e. results from test runs in the desktop test suite. This represents the objective part of the validation. The second and third part presents the subjective validation from initial test runs in the actual simulator and results from the study.

6.1 Simulation results

To generate suitable input signals to the test environment, test runs are made in Sim IV with the motion system disconnected. The generated signals from the vehicle model are then used to test the preposition algorithm in the desktop environment. The different test runs used in the desktop simulations and which were used to create the plots in this chapter are briefly described in Table 6.1.

Table 6.1: Test runs

No.	Description	Used to test
1	High accelerations and braking on straight road	pp_x
2	Drive on curvy road	pp_y
3	Drive on curvy road with brakes and accelerations	pp_x and pp_y

Drive No. 1 was made to test the longitudinal prepositioning and is therefore characterized by a number of accelerations and brakes. Drive No. 2 was made to test lateral prepositioning and was therefore driven on a part of a curvy test track. The layout of the track is available in Appendix A. Drive No. 3 was made to test the combined lateral and longitudinal prepositioning. Vehicle accelerations and velocity profiles of the test runs are available in Appendix C. The parameters of the prepositioning unit are tuned to avoid hitting the boundaries as if the motion system was connected. The tuning was done using several different test runs and roads and with varying degree of hard driving. The tuning of these parameters are always a trade off, driving to recklessly with any settings will lead to boundaries being hit. The parameter settings can be found in Appendix D. For clarity, the longitudinal and

lateral prepositioning algorithms are tested and the result are presented individually in this section.

6.1.1 Tests of longitudinal prepositioning

The longitudinal prepositioning, which uses the current velocity of the vehicle as input, is initially simulated with a test signal which represent a series of acceleration inputs to the MCA. Secondly signals from test run No. 1, with a series of heavy accelerations and brakes, are used.

Figure 6.1 show the pulse response in the motion cueing algorithm, with and without the longitudinal prepositioning active. The pulses corresponds to a five second acceleration at time ten seconds, and a five second braking manoeuvre at time 40 seconds. Figure 6.1a show a slight increase in sled acceleration, both in magnitude and duration. In Figure 6.1b one can clearly see the prepositioning displacement to a negative offset in the beginning and the increased displacement expressed in the sled due to lowered ω_{lf} .

Figure 6.2a shows a comparison between an acceleration represented in the x,y -sled with and without prepositioning in a six second portion of test run No. 1. Here one can clearly see the increase in the accelerations rendered in the sled as a result of lowered ω_{lf} . Figure 6.2b illustrates the decrease and delay in tilt coordination introduced with lowered ω_{lf} for longitudinal accelerations during 60 seconds of test run No. 1.

It is evident that both the established criteria in the beginning of the chapter are met; more accelerations are represented in the sled and less in tilt coordination. The tilt coordination come later into play and the tilt rate, i.e. the slope of the curve in Figure 6.2b, is lower when the prepositioning algorithm is active. The peak tilt rates at the different test runs are further discussed later in this section.

The possibility to represent more acceleration in the sled, i.e. lowering ω_{lf} results in larger motions which without prepositioning would lead to the sled reaching its boundaries. Figure 6.3 shows the longitudinal position of the sled during the whole test run 1. With the prepositioning algorithm turned off the sled stays within its boundaries but with prepositioning off the boundaries are hit. Both signals in this plot were generated with the same, lowered ω_{lf} .

The increase in total and maximum acceleration rendered in the x,y -sled and decrease in tilt coordination compared with prepositioning off are presented in Table 6.2, where

$$a_{Sd,x,tot} = \sqrt{\frac{t_s}{T} \sum_{0 \leq t_s < T} a_{Sd,x}(t_s)^2}, \quad (6.1)$$

which is the root mean square, RMS, a measure of the magnitude change of a varying

signal, and

$$a_{Sd,x,max} = \max(a_{Sd,x}), \quad (6.2)$$

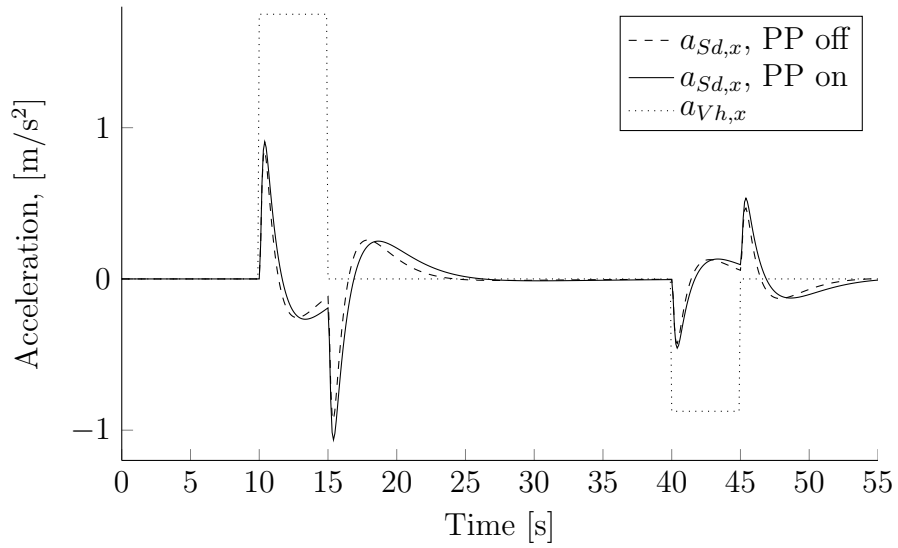
and

$$\omega_{TC,max} = \max(\omega_{TC}). \quad (6.3)$$

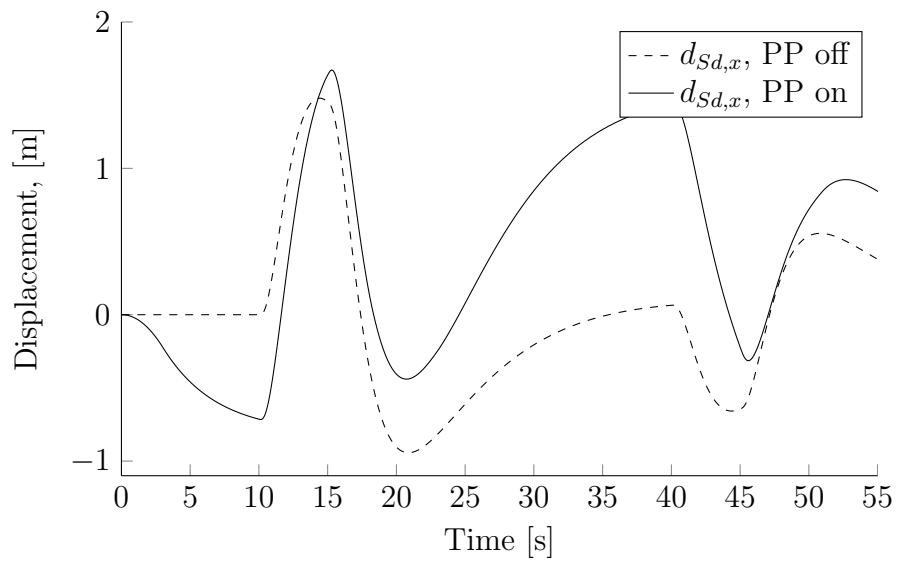
A increase in $a_{Sd,x,tot}$ by 25 % together with a decrease in the peak tilt rate by almost 30 % can be seen.

Table 6.2: Results, Drive No. 1

	Unit	PP off	PP on	Change
$a_{Sd,x,tot}$	m/s ²	0.176	0.220	+25 %
$a_{Sd,x,max}$	m/s ²	0.919	0.998	+9 %
$\omega_{TC,max}$	°/s	7.20	5.05	-29.9 %

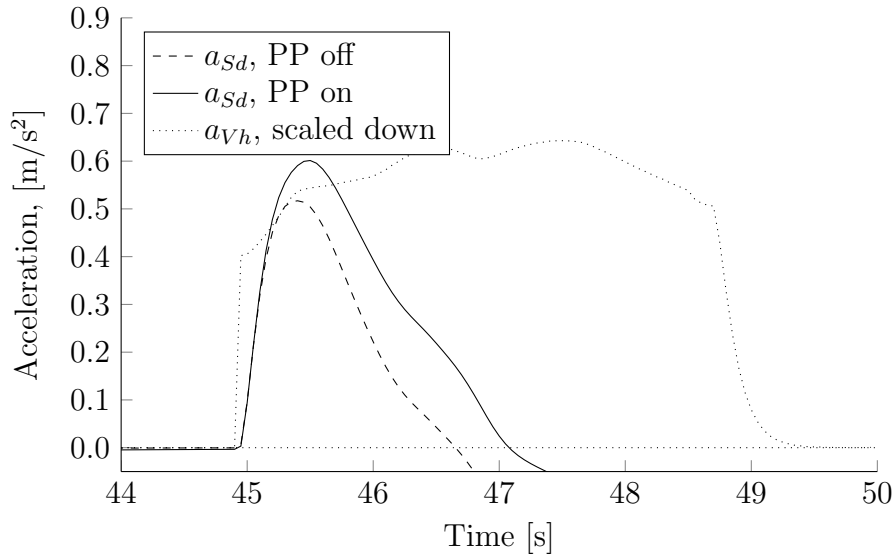


(a) Acceleration response of acceleration pulse.

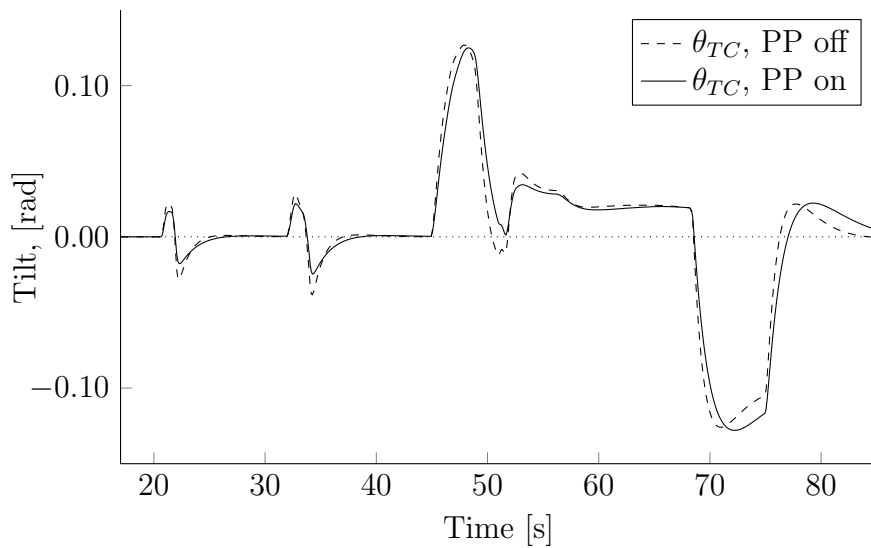


(b) Position response of acceleration pulse.

Figure 6.1: Sled acceleration and displacement response of vehicle acceleration pulse in MCA.



(a) $a_{Sd,x}$ and $a_{Vh,x}$ with and without prepositioning. 6 s portion of drive No. 1



(b) θ_{TC} with and without prepositioning. 60 s of drive No. 1.

Figure 6.2: Representation of accelerations in (a) sled and (b) tilt coordination with and without PP.

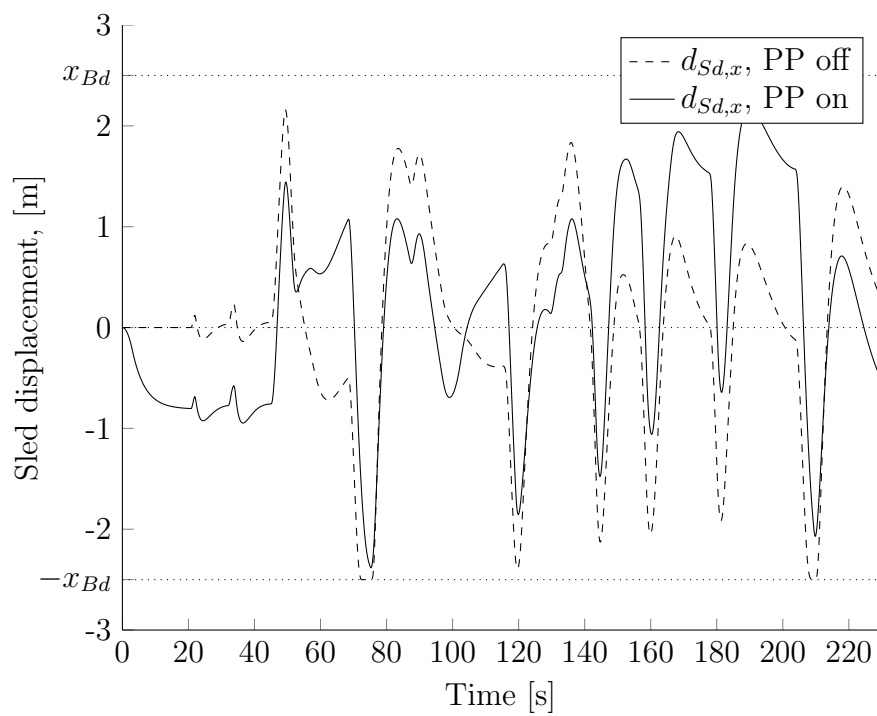


Figure 6.3: Longitudinal position of sled comparison with and without prepositioning. x,y -sled hitting its boundaries. Drive No. 1.

6.1.2 Tests of lateral prepositioning

An initial test is done with a step response of the curvature C while driving at a constant longitudinal vehicle velocity, v_{Vh} . The corresponding step in lateral acceleration of the vehicle as well as the accelerations represented by the sled with and without prepositioning is seen in Figure 6.4a. Figure 6.4b show the lateral displacements in the sled from this manoeuvre. It is evident that the sled start to preposition at time 30 s for the upcoming curvature.

Further testing of the lateral prepositioning, which is based on prediction of lateral accelerations based on future road data, is done in a very curvy, race track like, road. The layout of the road segment used in this test is seen in Figure A.1 in Appendix A. The total vehicle acceleration and velocity profile of the test run is seen in Figures C.3 and C.4.

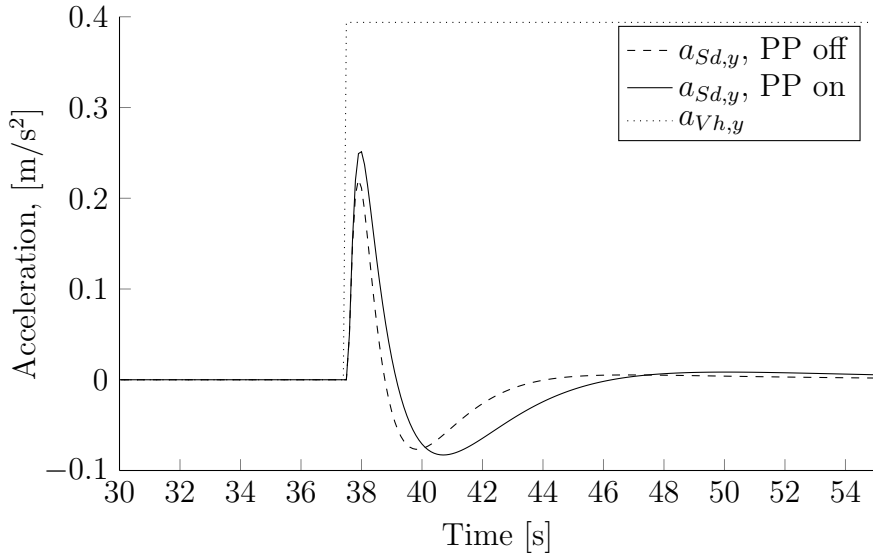
In Figure 6.5 a part of the run is shown. As one can see there are both higher and longer sustained acceleration when the prepositioning is used. Note that when prepositioning is on a lower cut off frequency ω_{lf} is used. The accelerations from the prepositioning algorithm is subtracted from the sled accelerations in the plot to illustrate only the desired accelerations.

Using the lower ω_{lf} with the prepositioning off the sled hits the boundary, see Figure 6.6. This occurred during the extended curve in the bottom of Figure A.1 in Appendix A.

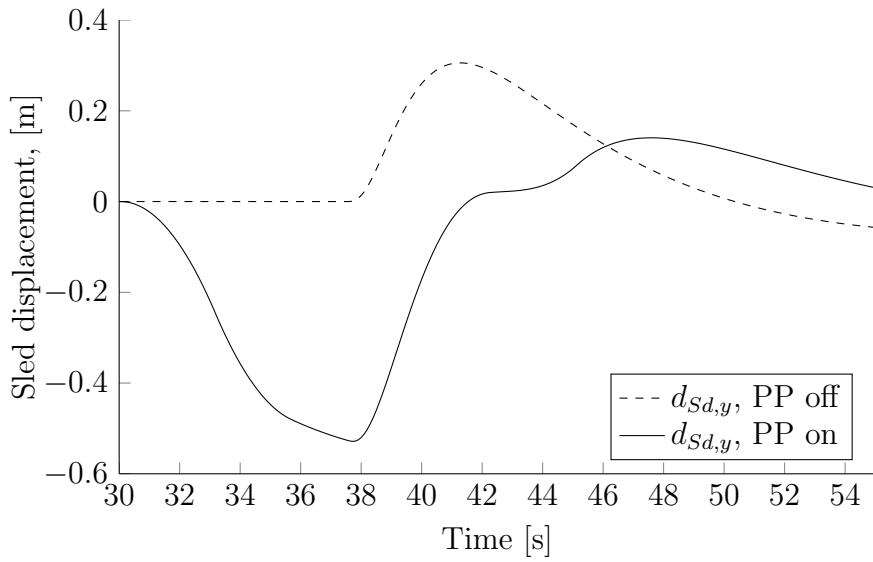
The increase in total and maximum accelerations rendered in the x,y -sled and decrease in maximum tilt coordination compared with prepositioning off are presented in Table 6.3. $a_{Sd,tot}$, $a_{Sd,max}$ and $\omega_{TC,max}$ as per Equations 6.1, 6.2 and 6.3.

Table 6.3: Results, Drive No. 2

	Unit	PP off	PP on	Change
$a_{Sd,y,tot}$	m/s ²	0.047	0.072	+53 %
$a_{Sd,y,max}$	m/s ²	0.328	0.397	+21 %
$\omega_{TC,max}$	°/s	4.45	3.55	-20.2 %



(a) Acceleration response of road curvature step.



(b) Position response of road curvature step.

Figure 6.4: Sled acceleration and displacement response of road curvature C step in lateral prepositioning algorithm. Vehicle velocity, v_{Vh} is constant.

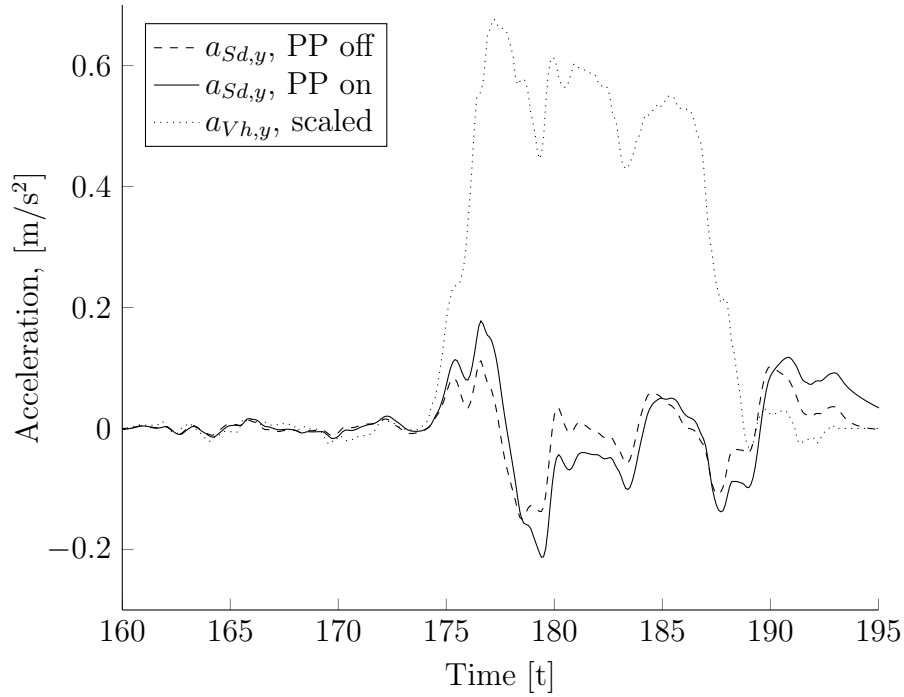


Figure 6.5: Lateral acceleration comparison with and without prepositioning. Drive No. 2. Vehicle acceleration scaled by MCA scaling factor.

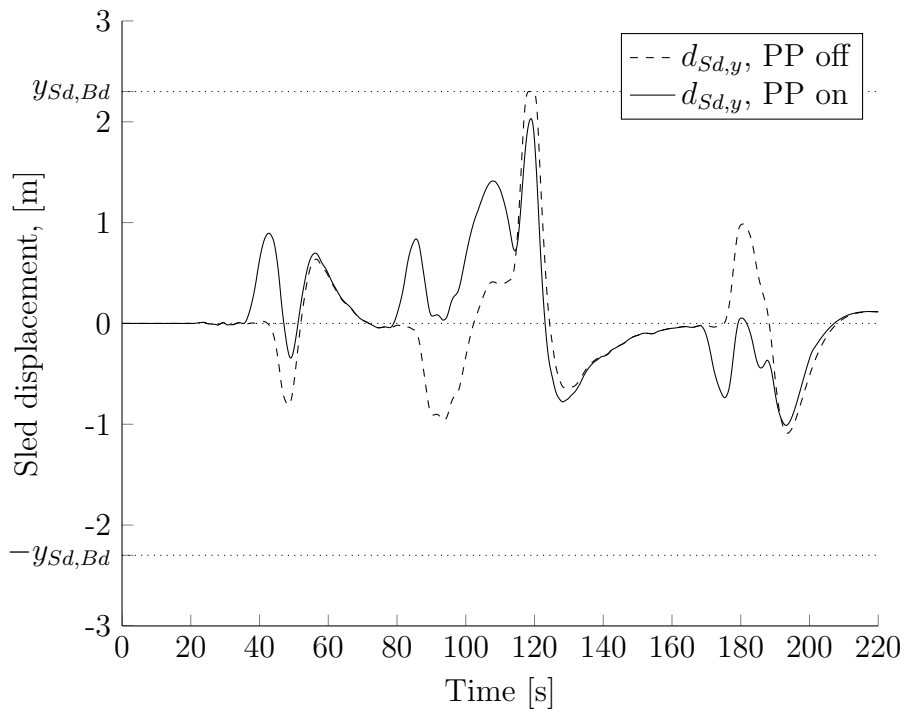


Figure 6.6: Lateral position of sled comparison with and without prepositioning, boundary hit. Drive No. 2.

6.1.3 Test of total prepositioning

Test run No. 3 was made in order to evaluate concurrent lateral and longitudinal prepositioning. The test road was the same as in test run No. 2, Appendix A, and the setup was similar but with the addition of a number of extra brakes and accelerations. The vehicle acceleration and velocity profile of the test run can be found in Appendix C.

The increase in total and maximum accelerations rendered in the x,y -sled and the maximum tilt rate, in any direction, compared with prepositioning off are presented in Table 6.4. $a_{Sd,tot}$, $a_{Sd,max}$ and $\omega_{TC,max}$ as per Equations 6.1, 6.2 and 6.3.

Table 6.4: Results, Drive No. 3

	Unit	PP off	PP on	Change
$a_{Sd,x,tot}$	m/s ²	0.243	0.267	+10 %
$a_{Sd,y,tot}$	m/s ²	0.047	0.067	+44 %
$a_{Sd,x,max}$	m/s ²	1.003	1.095	+9 %
$a_{Sd,y,max}$	m/s ²	0.342	0.451	+32 %
$\omega_{TC,max}$	°/s	8.05	6.33	-21 %

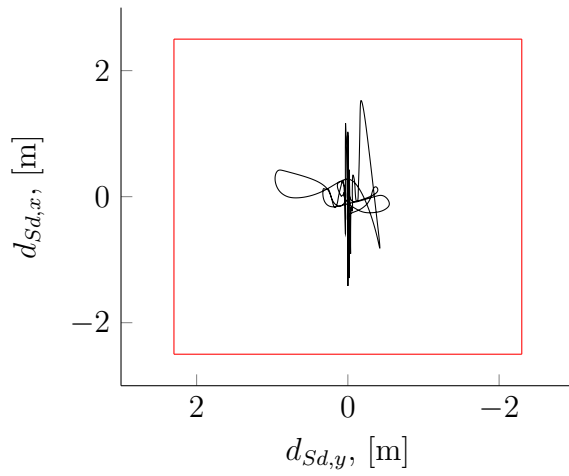
To better visualise the effects of both prepositioning and the change in ω_{lf} , plots of the sled displacement in both longitudinal and lateral direction during the entire test run is shown in Figures 6.7a, 6.7b and 6.7c. It is clear from these plots that the sled is better utilised when the prepositioning is used.

6.2 Initial test drives

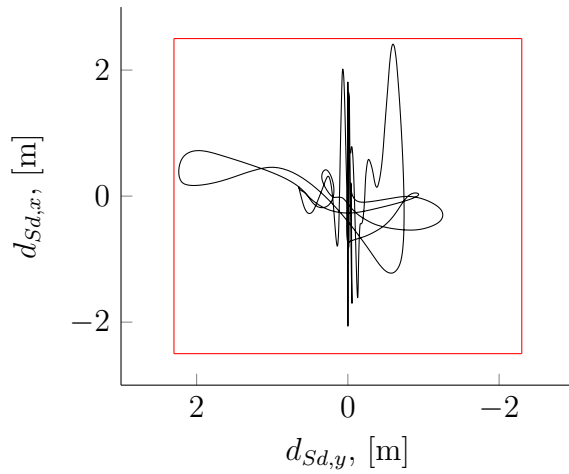
The first tests of the prepositioning algorithm in the simulator with the motion system turned on were initially performed with ω_{lf} set to the original settings, found in Table D.1 in Appendix D. This was done as a precaution to make sure that the simulator motion boundaries were respected. After this, the ω_{lf} was gradually changed to the final values, also found in found in Table D.1.

The roads used during the initial tests with the motion system activated were the same as in Section 6.1. The curvy road, although with the rendered motion already simulated in the test suite, was deemed to be too uneven for further testing. It contains banking and slopes that causes the hexapod to, in some situations, work to close to its boundaries and even sometimes reaching them. Unexpected manoeuvres during a drive might cause such boundary violations. The layout of this road is available in Appendix A.

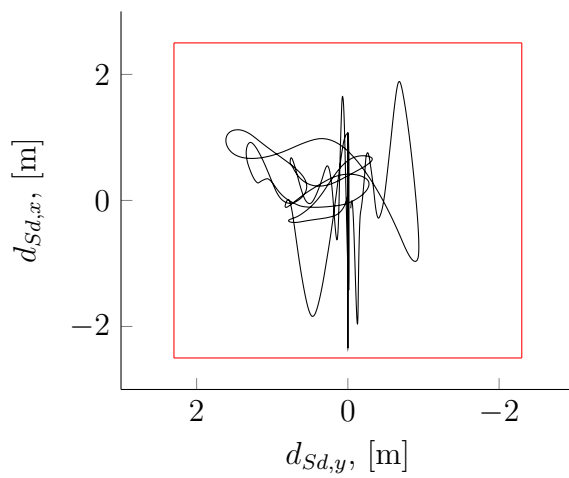
In order to investigate the necessity of a limitation of the jerk in the prepositioning



(a) Sled displacement, original MCA, standard ω_{lf} .



(b) Sled displacement, original MCA, lowered ω_{lf} , near boundary hits.



(c) Sled displacement, original MCA, lowered ω_{lf} + PP.

Figure 6.7: x,y -plot of sled displacement during drive No. 3.

motion it was in the initial test runs inactivated entirely and only the acceleration limitation was active. Three different drivers, the two authors and their instructor, all reported sensing a jerk at the beginning and end of the lateral repositioning but could not detect any motion in between. It was thus decided to activate the jerk limitation to allow a maximum of $\dot{j}_{lim} = 0.1 \text{ m/s}^3$. All three drivers did subsequent test runs and all reported that the jerk had disappeared. It is thus in this short initial study concluded that the detectable motion of the repositioning had been either removed entirely or been sufficiently masked among other disturbances and sensory cues.

6.3 Study

As mentioned earlier, since the perceived validity or realism of any simulator depend on human perception there is no good objective way to measure it but to let unbiased test subjects drive and validate the simulator [4, 12, 34]. The experiment presented here is in form of a psychophysical face validation designed to fully test if the introduced repositioning features actually improves the realism.

12 test subjects were asked to drive in the simulator two times each, alternating with or without repositioning. Directly after both test runs they were asked to evaluate it based on their previous, real-life driving experience.

The test scenario was exactly the same for both test runs; The road is of type "Swedish rural road" and starts with a straight and finishes with a series of turns, the layout of the road and the key events are available in Appendix B. The test subjects were asked to start driving at 50 km/h. After 1.0 km they were asked to increase speed to 70 km/h. After 1.6 km they were asked to stop the car entirely and then resume driving at 50 km/h. After 2.0 km the road becomes "curvier" and after 4.3 km the test subjects were asked to stop the car. Each test run took about five minutes to complete.

Immediately after both runs, the test subjects were given a questionnaire, available in Appendix E. They were asked to rate accelerations, braking, turning, if they felt any unprovoked motion and if they experienced any motion sickness on a scale of 1-7.

The real questions answered indirectly with the questionnaire were:

- Does the increased motion rendering in the x,y -sled increase the validity or realism of the simulator? Questions 5-7 and 11-13.
- Is the repositioning motion perceivable? Questions 8 and 14.
and
- Does the increased motion rendering in the x,y -sled reduce motion sickness? Questions 9 and 15.

The main results from the study are presented in Table 6.5. It shows the mean result on each question with and without prepositioning and the difference between the two. The entire questionnaire result is found in Appendix F.

At a first glance there appears to be an improvement in all five categories with the prepositioning turned on. Note that in columns 1-3 a positive difference means an improvement while in columns 4-5 a negative difference means an improvement of the simulator.

A statistical verification to ensure if any real difference can be shown is done with a paired t-test. The paired t-test is used to evaluate if two data sets are significantly different [35]. It is found that at a 95% confidence interval there are statistically significant differences between the case with and without prepositioning in questions 5 & 11, regarding the realistic feel of acceleration, and in questions 6 & 12, regarding the realistic feel of the braking. Unfortunately statistically significant differences could not be established for questions 7 & 13, regarding turning, questions 8 & 14, regarding unprovoked motion or for questions 9 & 15, regarding motion sickness. Although the mean values and their differences are equal for the second and third question the test for statistical significance shows different results. This is due to difference in the standard deviation between the samples which come into play when calculating statistical significance, the standard deviations can be found in Appendix F. Since the differences is quite small further tests are necessary in order to establish statistical significance.

Table 6.5: Questionnaire results, mean scores

Question No.	5/11	6/12	7/13	8/14	9/15
Mean score PP on	5,58	5,33	4,83	2,58	2,83
Mean score PP off	4,50	4,83	4,33	2,92	3,17
Difference	1.08	0.50	0.50	-0.34	-0.34

7 Discussion

Both simulations and real tests show that the prepositioning algorithm presented in this thesis works as intended; it finds an offset preposition both in lateral and longitudinal direction and it moves the x,y -sled to that point, in time for the subsequent motion, below the human perception threshold. The study also give evidence of an increased realism in the longitudinal motion, i.e. in acceleration and braking. There are also indications of increased realism in the lateral movements but statistical significance at a high enough level could not be established. Further testing is needed.

Although, as always, some improvements are possible. Apart from the 60 possible parameters available in the current motion cueing algorithm, there is a new set of parameters introduced with the prepositioning algorithm that can be tuned to improve the functionality. Tuning parameters in this type of simulator is hard and time consuming but there is a potential high gain of a well tuned simulator. Due to the quite limited time frame of this project, not much time has been spent in this area.

The possibility to virtually expand the motion envelope of a motion system with a classic motion cueing algorithm and prepositioning has been discussed. The changing of cut-off frequencies in washout filters can be made time varying. In this way the simulator can adapt to the current driving situation and always maximise its motion envelope. On-line changing of cut off frequencies can however lead to some undesirable behaviour if not implemented correctly. Simply making discrete altering of the cut off frequency will lead to discontinuous step like effects in the outputs of the filters. Lorenz et al. [36] suggest an algorithm which will eliminate the discontinuities in the filter outputs. This method however involves a rather in depth alteration of the configuration of the motion cueing system. Another possible drawback of on-line frequency changes is that the motion cues become inconsistent since the same manoeuvre can be represented differently depending on the current state of the simulator motion system.

Another approach for longitudinal prepositioning, which could also be used in combination with the above described method, is to analyse the road database in a similar fashion as with the lateral prepositioning. The road itself does not contain any specific speed, one can drive as fast or as slow as either the vehicle or the driver can manage. Neither does the road database contain a specific speed. The likelihood of someone driving at the current speed limit or at a speed suiting the current type of road has to be considered. The algorithm can look for road signs indicating speed limits or evaluate the type of road by counting lanes, curvature etc. and prepare the simulator for a possible driving scenario. This approach is outside the scope for this thesis.

The lateral prepositioning algorithm assumes that the driver follows the same lane and only works for the upcoming curvature of that lane. If the road ahead contains

multiple lanes that branch out in different direction, slip roads etc. the prepositioning algorithm acts only for the current lane. Although a drivers decisions are hard to predict, a statistical probability can be used to preposition the simulator to accommodate all possible future movements.

The velocity input to the lateral prepositioning subsystem is assumed to be constant. I.e. the driver is assumed to keep the same velocity during the entire t_h . This is likely not the case in most situations, as drivers with some self-preservation unarguably lower their vehicle velocity before upcoming sharp curves. This is an area that needs to be investigated further in a future implementation.

References

- [1] *VTI simulator facilities*. (2014-06-24). VTI. URL: <http://www.vti.se/en/research-areas/vehicle-technology/vtis-driving-simulators/>.
- [2] Martin Fischer, Håkan Sehhammer, and Göran Palmkvist. “Motion cueing for 3-, 6-and 8-degrees-of-freedom motion systems”. *Proceedings of the Driving Simulation Conference Europe 2010*. 2010.
- [3] Martin Fischer, Håkan Sehhammer, and Göran Palmkvist. Applied motion cueing strategies for three different types of motion systems. *Journal of Computing and Information Science in Engineering* **11.4** (2011), 041008.
- [4] Martin Fischer, Lars Eriksson, and Katharina Oeltze. Evaluation of methods for measuring speed perception in a driving simulator. *Actes INRETS* (2012), 71–93.
- [5] Thomas Chapron and Jean-Pierre Colinot. “The new psa peugeot-citroen advanced driving simulator overall design and motion cue algorithm”. *Proceedings of Driving Simulation Conference*. 2007.
- [6] Cornelius Weiß. “Control of a Dynamic Driving Simulator: Time-Variant Motion Cueing Algorithms and Prepositioning”. MA thesis. Deutschen Zentrum für Luft und Raumfahrt, 2006.
- [7] MATLAB Simulink. *multiple versions*.
- [8] Andrew Hamish John Jamson. Motion cueing in driving simulators for research applications (2010).
- [9] M Pinto, V Cavallo, and T Ohlmann. The development of driving simulators: toward a multisensory solution. *Le travail humain* **71.1** (2008), 62–95.
- [10] Imad Al Qaisi and Ansgar Traechtler. “Constrained Linear Quadratic Optimal Controller for Motion Control of ATMOS Driving Simulator”. *Driving Simulation Conference*. 2012.
- [11] F Colombet et al. “Motion cueing: What is the impact on the driver’s behavior”. *Proceedings of the Driving Simulation Conference*. 2008, pp. 171–181.
- [12] Per Henriksson. Simulatorsjuka-orsak, verkan och åtgärder: en kunskapsöversikt (2009).
- [13] Jean-Michel Auberlet et al. The impact of perceptual treatments on lateral control: A study using fixed-base and motion-base driving simulators. *Accident Analysis & Prevention* **42.1** (2010), 166–173.
- [14] Yeong Shiong Chiew, Mohamad Kasim Abdul Jalil, and Mohamed Hussein. “Motion cues visualisation of a motion base for driving simulator”. *Robotics and Biomimetics, 2008. ROBIO 2008. IEEE International Conference on*. IEEE. 2009, pp. 1497–1502.
- [15] EF Fichter, DR Kerr, and J Rees-Jones. The Gough—Stewart platform parallel manipulator: A retrospective appreciation. *Proceedings of the Institution of Mechanical Engineers, Part C: Journal of Mechanical Engineering Science* **223.1** (2009), 243–281.
- [16] *Encyclopedia Britannica Online*. <http://www.britannica.com/>. (2014-06-24). Web, 2014.

- [17] AJ Benson, MB Spencer, and JR Stott. Thresholds for the detection of the direction of whole-body, linear movement in the horizontal plane. *Aviation, space, and environmental medicine* (1986).
- [18] EL Groen and W Bles. How to use body tilt for the simulation of linear self motion. *Journal of Vestibular Research* **14.5** (2004), 375–385.
- [19] Alessandro NESTI et al. Roll rate thresholds and perceived realism in driving simulation. *Actes INRETS* (2012), 23–31.
- [20] Nikolce Murgovski. Vehicle modelling and washout filter tuning for the chalmers vehicle simulator. *Lund University, IEA* (2007).
- [21] LD Reid and MA Nahon. *Flight Simulation Motion-base Drive Algorithms: Part 1-Developing and Testing the Equations*. Institute for Aerospace Studies, Toronto University, 1985.
- [22] Bruno Augusto and Rui Loureiro. Motion cueing in the Chalmers driving simulator-A model predictive control approach (2009).
- [23] Russell V Parrish, James E Dieudonne, and Dennis J Martin Jr. Coordinated adaptive washout for motion simulators. *Journal of Aircraft* **12.1** (1975), 44–50.
- [24] Raphael Sivan, Jehuda Ish-Shalom, and Jen-Kuang Huang. An optimal control approach to the design of moving flight simulators. *Systems, Man and Cybernetics, IEEE Transactions on* **12.6** (1982), 818–827.
- [25] *EMotion-2500-8DOF-500-MK2-XY System Description*. Rexroth Bosch Group. 2010.
- [26] Jorge Gómez Fernández. A Vehicle Dynamics Model for Driving Simulators (2012).
- [27] *The OpenDRIVE® project*. (2014-06-24). URL: <http://www.opendrive.org/>.
- [28] Marius Dupuis et al. *OpenDRIVE Format Specification®*, Rev. 1.3. 1.3. VIRES Simulationstechnologie GmbH. 2013.
- [29] *Euler spiral*. (2014-06-24). URL: http://en.wikipedia.org/wiki/Euler_spiral.
- [30] Bruce Haycock and Peter R Grant. “The influence of jerk on perceived simulator motion strength”. *Driving Simulation Conference*. 2007.
- [31] *Internal Sim IV documents*. VTI Intranet.
- [32] Martin Fischer. *Motion-Cueing-Algorithmen für eine realitätsnahe Bewegungssimulation*. Deutsches Zentrum für Luft-und Raumfahrt in der Helmholtz-Gemeinschaft, DLR, 2009.
- [33] Peter Hippe. Eine systematische Vermeidung der durch Stellbegrenzungen ausgelösten Probleme. *at-Automatisierungstechnik* **55.8** (2007), 377–393.
- [34] Andras Kemeny and Francesco Panerai. Evaluating perception in driving simulation experiments. *Trends in cognitive sciences* **7.1** (2003), 31–37.
- [35] J.H. McDonald. *Handbook of Biological Statistics (2nd ed.)* Sparky House Publishing, Baltimore, Maryland, 2009.
- [36] Tobias Lorenz, Klaus Jaschke, and Frank Köster. Motion Cueing Algorithm Online Parameter Switching in a Blink of an Eye—A Time-Variant Approach. *Journal of Computing and Information Science in Engineering* **11.4** (2011), 041002.

A Test road "Curvy test track"

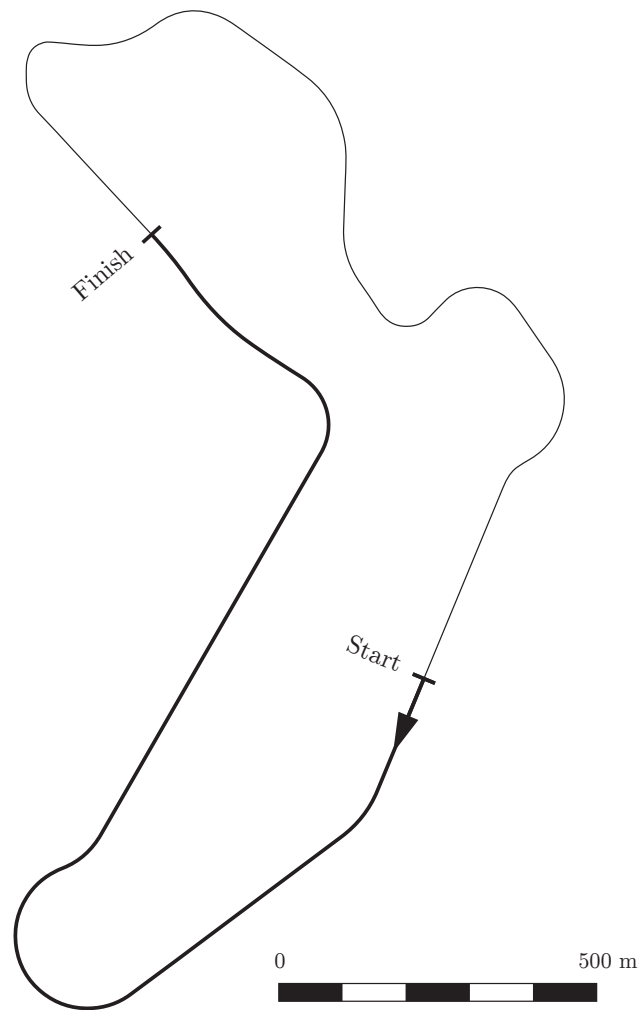


Figure A.1: Test road "Rural"

B Test road "Swedish rural road"

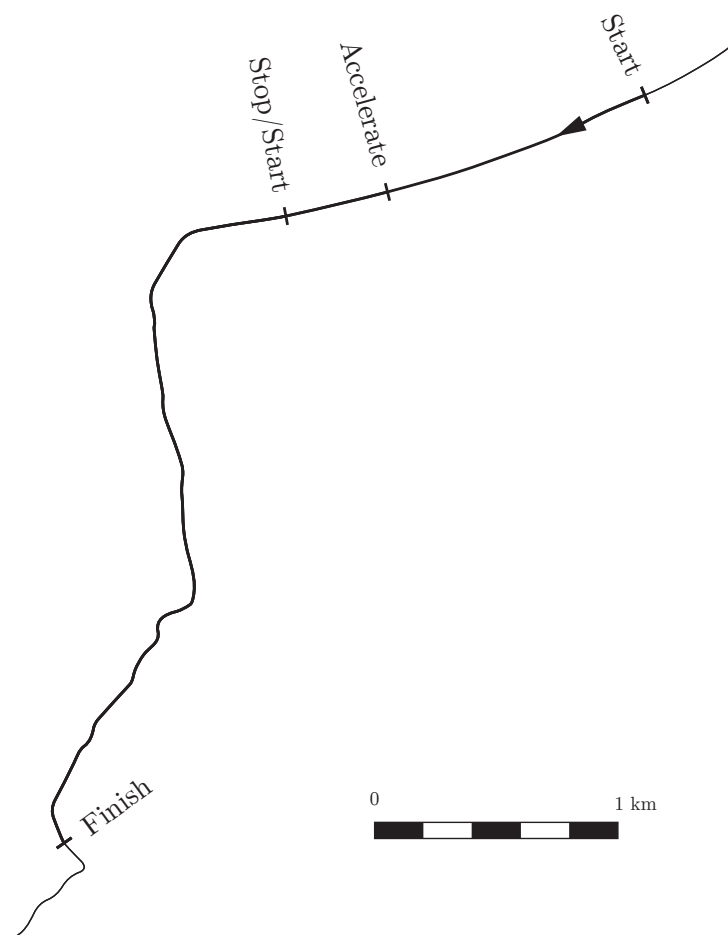


Figure B.1: Test road "Swedish rural road"

C Test run profiles

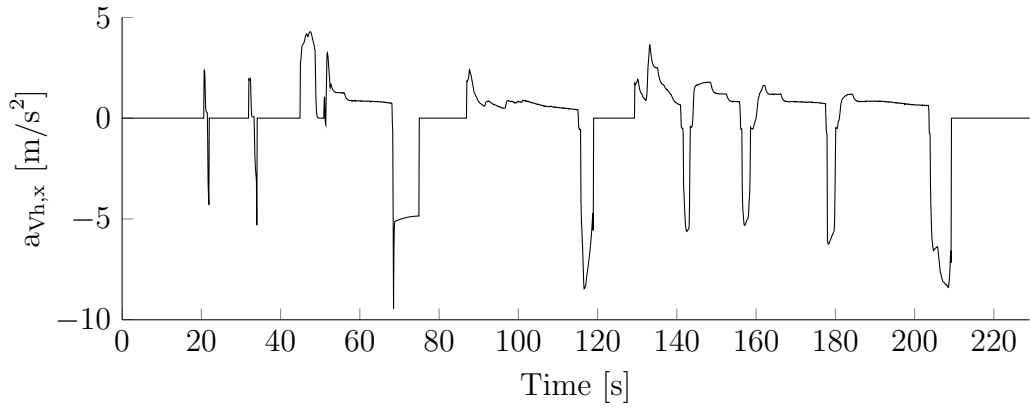


Figure C.1: Drive No. 1, $a_{Vh,x}$ profile

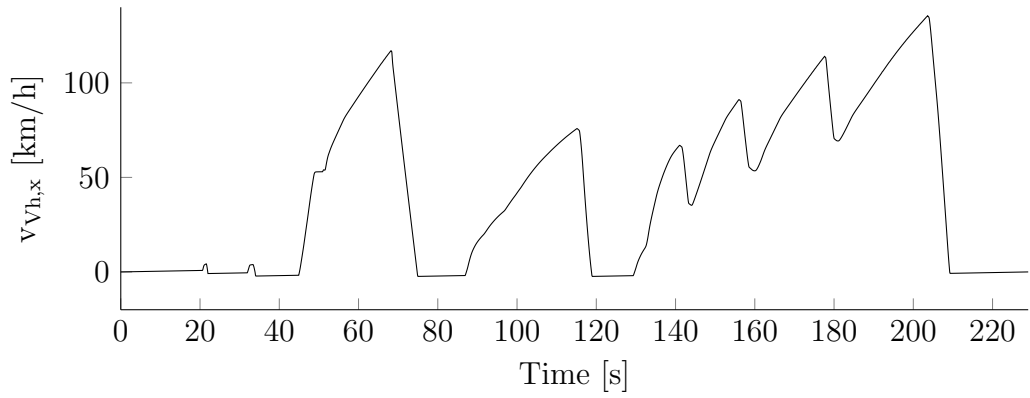


Figure C.2: Drive No. 1, $v_{Vh,x}$ profile

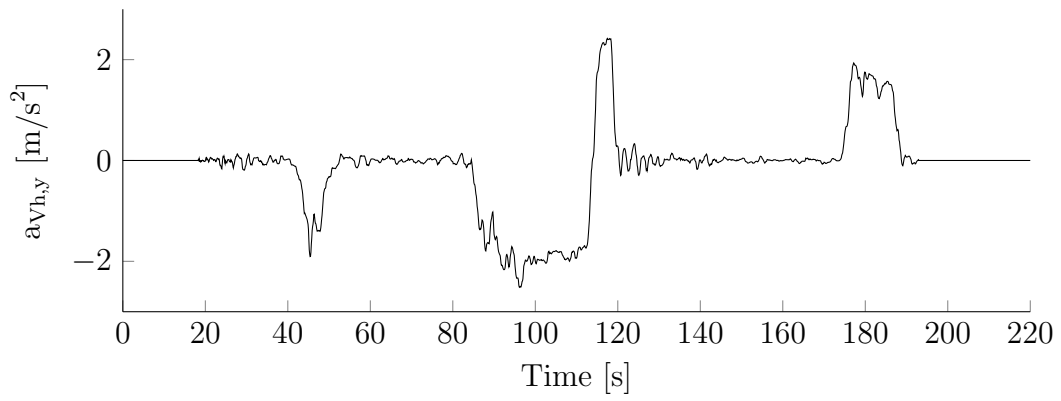


Figure C.3: Drive No. 2, $a_{Vh,y}$ profile

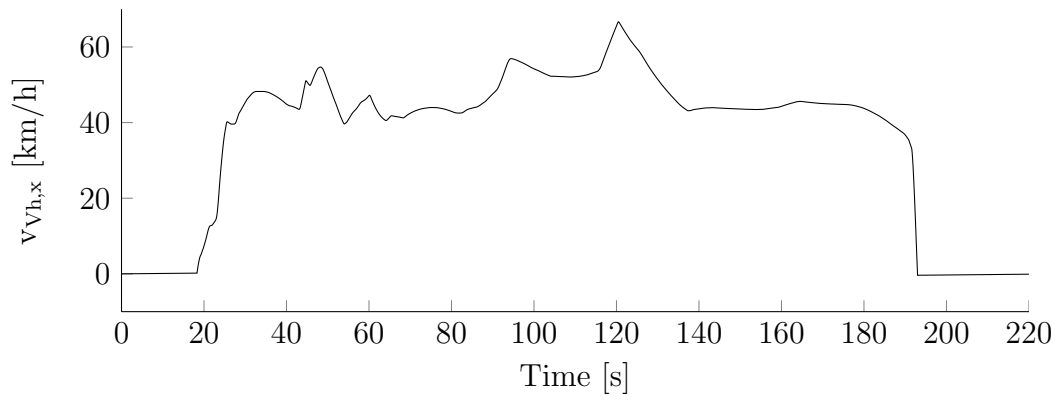


Figure C.4: Drive No. 2, $v_{Vh,y}$ profile

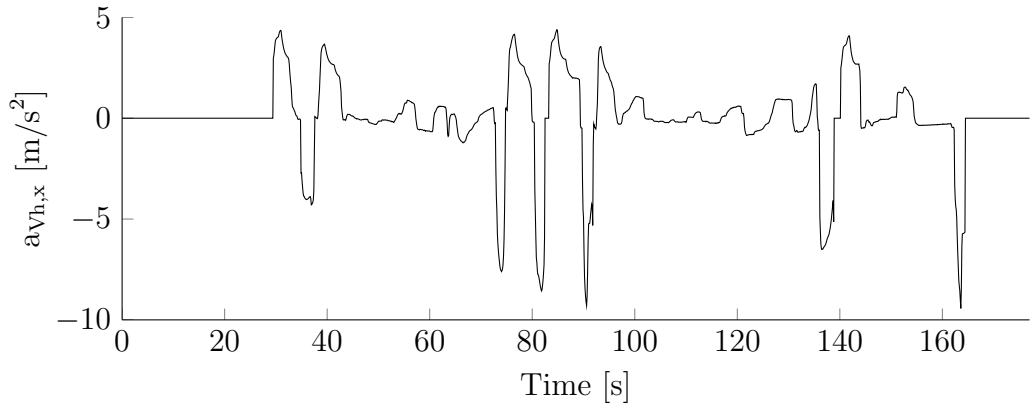


Figure C.5: Drive No. 3, $a_{Vh,x}$ profile

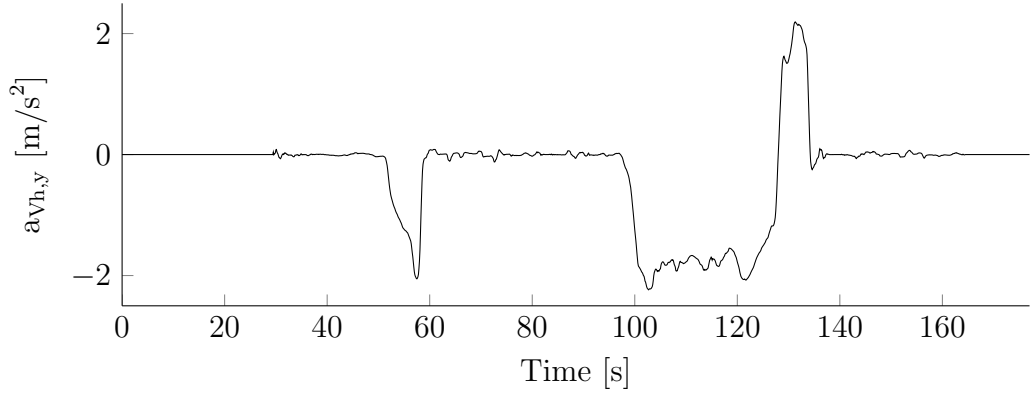


Figure C.6: Drive No. 3, $a_{Vh,y}$ profile

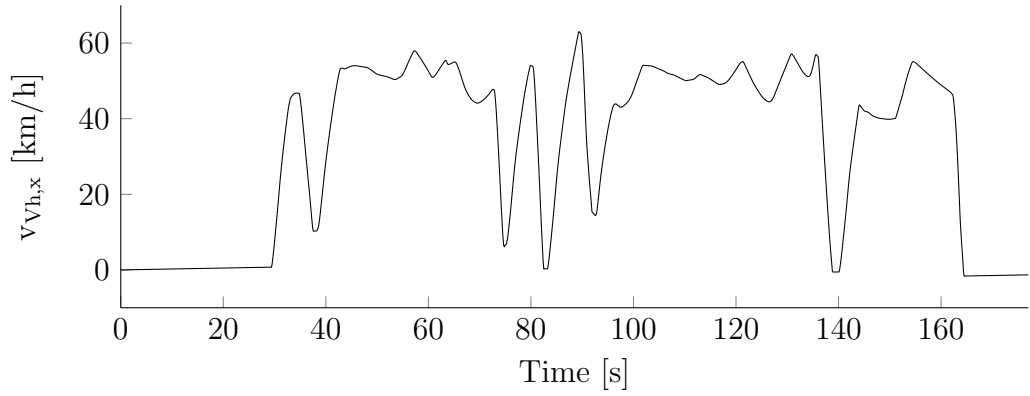


Figure C.7: Drive No. 3, $v_{Vh,x}$ profile

D Parameter settings

Table D.1: Parameters

Param.	PP=on/off	Unit	List name*	Description
t_h	15/-	s	n/a	The pp_y time horizon, the time ahead where the PP algorithm collects curvature data.
$x_{pp,min}$	-1.1/-	m	n/a	The longitudinal prepositioning boundaries. Can be scaled and offset.
$x_{pp,max}$	1.5/-	m	n/a	The longitudinal prepositioning boundaries. Can be scaled and offset.
$x_{pp,min}$	0.3/-	m	n/a	The offset of x_{pp} .
$y_{pp,lim}$	1/-	m	n/a	The lateral prepositioning boundaries.
a_{lim}	0.05/-	m/s ²	n/a	Limit of prepositioning acceleration.
\dot{j}_{lim}	0.1/-	m/s ³	n/a	Limit of prepositioning jerk.
P	0.05/-	-	n/a	P-value of PD-controller of a - and j limiter.
D	3.075/-	-	n/a	D-value of PD-controller of a - and j limiter.
k	50	-	n/a	Jerk limiter inner loop gain
$\omega_{lf,x}$	0.55/0.65	rad/s	xMCwLf	Cut-off frequency of filter, PP off.
$\omega_{lf,y}$	0.55/0.85	rad/s	yMCwLf	Cut-off frequency of filter, PP off.

*The name of the parameter in the parameter list used in Sim IV.

F Study results

”About you” data

Subject No.	PP drive	Date	Age	km/year*	Vehicles	Prev. Sim drives
1	1	03-06-2014	39	2	car, MC	>3
2	2	03-06-2014	24	1	car	0
3	1	03-06-2014	20	1	car	0
4	2	03-06-2014	29	3	car	0
5	1	03-06-2014	30	2	car	0
6	2	03-06-2014	31	1	car	0
7	1	03-06-2014	30	1	car	0
8	2	04-06-2014	61	3	car	0
9	1	04-06-2014	35	1	car	0
10	2	04-06-2014	33	1	car	2-3
11	1	04-06-2014	31	1	car	0
12	2	04-06-2014	33	2	car	0

* (1 = ”0 - 10 000”, 2 = ”10 000 - 20 000” and so on.)

Results data The questions are renamed A to K because of the sorting. A-E: PP on, G-K: PP off.

Subject No.	A	B	C	D	E	G	H	I	J	K
1	5	2	5	2	2	4	2	2	5	4
2	6	4	4	2	1	5	3	5	1	1
3	5	6	5	4	1	5	6	5	4	2
4	5	4	5	3	4	3	4	5	3	3
5	7	7	5	2	3	7	7	5	3	3
6	7	7	6	5	3	6	6	4	3	4
7	6	4	5	2	4	6	4	5	2	4
8	7	6	6	2	2	5	5	6	2	2
9	7	7	6	2	3	5	5	4	4	4
10	6	6	3	3	1	2	5	5	4	1
11	2	6	2	1	5	2	6	2	1	6
12	4	5	6	3	5	4	5	4	3	4
Total score	67	64	58	31	34	54	58	52	35	38
Mean score	5,58	5,33	4,83	2,58	2,83	4,50	4,83	4,33	2,92	3,17
STD	1,51	1,56	1,27	1,08	1,47	1,57	1,40	1,23	1,24	1,47

G Images



(a) Inside the dome



(b) Inside the car cabin

Figure G.1: Images of Sim IV